

THE UNIVERSITY OF MICHIGAN
COLLEGE OF ENGINEERING
Department of Electrical Engineering
Space Physics Research Laboratory

Scientific Report JS-1

THE DUMBBELL ELECTROSTATIC IONOSPHERE PROBE: THEORETICAL ASPECTS

W. R. Hoegy
L. H. Brace

ORA Projects 2816-1, 03484, and 03599

under contract with:

UNITED STATES AIR FORCE
AIR RESEARCH AND DEVELOPMENT COMMAND
AIR FORCE CAMBRIDGE RESEARCH LABORATORIES
GEOPHYSICS RESEARCH DIRECTORATE
CONTRACT NO. AF 19(604)6124
CAMBRIDGE, MASSACHUSETTS

DEPARTMENT OF THE ARMY
BALLISTIC RESEARCH LABORATORY
CONTRACT NO. DA-20-018-509-ORD-103
PROJECT NO. DA-5B03-06-011 ORD(TB3-0538)
ABERDEEN PROVING GROUND, MARYLAND

NATIONAL AERONAUTICS AND SPACE ADMINISTRATION
CONTRACT NO. NASw-139
WASHINGTON, D.C.

administered through:

OFFICE OF RESEARCH ADMINISTRATION ANN ARBOR

September 1961

PREFACE

This is the first of a series of three reports whose purpose is to document the theoretical and engineering aspects of the Dumbbell ionosphere probe and present the ionosphere data obtained through its use by University of Michigan researchers. This report describes the Dumbbell probe theory as it now exists. The second report, JS-2, treats the design and engineering of the Dumbbell, and a third report, JS-3, presents the data obtained in four flights and discusses it in the light of present ionosphere theories and the measurements by others. This research has been sponsored by Air Force Cambridge Research Center, U. S. Army Ordnance Ballistic Research Laboratories, and, more recently, by the National Aeronautics and Space Administration.

TABLE OF CONTENTS

	Page
ABSTRACT	v
LIST OF FIGURES	vii
LIST OF SYMBOLS	ix
1.0 INTRODUCTION	1
1.1 General Remarks Concerning the Design of an Ejectable Bipolar Probe	2
1.1.1 Theoretical Considerations	2
1.1.2 The Particular Ionospheric Parameter to be Measured	3
1.1.3 Rocket Vehicle Considerations	5
1.2 Selection of the Dumbbell Form of Probe	6
1.3 The Dumbbell Probe Instrument	8
2.0 GENERAL DISCUSSION AND PHYSICAL ASSUMPTIONS	15
2.1 Physical Assumptions Concerning the Earth's Ionosphere	15
2.2 The Positive Ion Sheath	15
2.3 The Effects of Probe Motion	17
2.4 The Mean Free Path of the Ions and Electrons	18
2.5 The Effect of the Earth's Magnetic Field	19
2.6 Photoemission Due to Solar Radiation	19
3.0 DERIVATION OF THE MOVING-HEMISPHERE CURRENT EQUATIONS	21
3.1 Random Positive Ion Current to a Dumbbell Hemisphere	21
3.2 Electron Current to a Dumbbell Hemisphere	24
3.3 The Net Hemisphere Current	25
3.4 The Relationship Between the Sheath Radius, a , and the Across-the-Sheath Potential, V	26
3.5 Final Form of the Net Hemisphere Current Equation	29
4.0 THE DUMBELL VOLT-AMPERE CHARACTERISTIC	L
5.0 THE METHOD OF ELECTRON TEMPERATURE REDUCTION FROM DUMBELL VOLT- AMPERE CHARACTERISTICS	37
6.0 THE METHOD OF REDUCING POSITIVE ION NUMBER DENSITY FROM DUMBELL VOLT-AMPERE CHARACTERISTICS	41

TABLE OF CONTENTS (Concluded)

	Page
7.0 CONCLUDING REMARKS	45
8.0 ACKNOWLEDGMENTS	47
9.0 REFERENCES	49
APPENDIX	
I. DERIVATION OF THE RANDOM CURRENT DENSITY TO A MOVING INFINITESIMAL AREA ELEMENT	51
II. THE RANDOM ION CURRENT TO A MOVING HEMISPHERE	52
III. ELECTRON CURRENT TO A HEMISPHERE	55
IV. DERIVATION OF THE SECOND ION CURRENT EQUATION THROUGH A SOLUTION OF POISSON'S EQUATION	56
V. RELATION BETWEEN PROBE POTENTIAL AND SHEATH RADIUS	58
VI. COMMENT ON THE EFFECT OF VELOCITY ON THE ELECTRON CURRENT	60

ABSTRACT

Some of the factors which enter into the selection of an ejectable, electrostatic, ionospheric probe configuration are discussed. The design of a particular probe, the Dumbbell, which was conceived and used by the authors and others,* is outlined. Equations for the ion and electron current to a moving hemispherical collector are developed and applied to predict the volt-ampere characteristics of the Dumbbell, a double-hemisphere probe. Several characteristics are shown graphically and discussed in terms of the effects of probe velocity. The methods by which the electron temperature and the positive ion density are derived from such volt-ampere characteristics are discussed.

*N.W. Spencer and R.L. Boggess, formerly with Space Physics Research Laboratory.

LIST OF FIGURES

Figure	Page
1. The Dumbbell instrument.	8
2. Partially disassembled Dumbbell.	9
3. Functional block diagram showing bipolar probe system.	11
4. Artist's conception of the ejection of the Dumbbell into the ionosphere.	13
5. Velocity factor of the random current density.	23
6. Velocity factor $\Lambda(\lambda, \theta)$ of random hemisphere current.	25
7. Single-hemisphere current curves for a fixed velocity and selected orientations.	29
8. Superposed current characteristics of two oppositely oriented hemispheres.	31
9. A particular Dumbbell orientation.	31
10. Volt-ampere characteristics of Dumbbell having orientation shown in Figure 9.	32
11. Dumbbell volt-ampere characteristics for $\theta = 0^\circ$ and selected velocity ratios.	33
12. Dumbbell volt-ampere characteristics for $\theta = 180^\circ$ and selected velocity ratios.	34
13. Dumbbell volt-ampere characteristics for $\theta = 90^\circ$ and selected velocity ratios.	35
14. Dumbbell volt-ampere characteristics for $\theta = 45^\circ$ and selected velocity ratios.	36
15. Dumbbell volt-ampere characteristics showing pertinent factors in the reduction of ionospheric parameters.	37
16. Hemisphere orientation.	53

LIST OF SYMBOLS

a	radius of positive ion sheath
a/r	ratio of sheath radius to probe radius
c_e	electron characteristic velocity
c_p	positive ion characteristic velocity [see Eq. (3.3)]
e	unit charge = 1.60206×10^{-19} coulombs
i_e	electron current
i_{neg}	current due to negative ions
i_p	positive ion current
i_{photo}	current due to photoemission
j_x	current density in x direction
k	Boltzmann constant = 1.38044×10^{-23} joules/degree K
M	mass number
m_e	electron mass = 9.1083×10^{-31} kg.
m_p	positive ion mass = $1.660 M \times 10^{-27}$ kg
N_e	electron number density
N_p	positive ion number density
P	$P = \frac{8 \sqrt{\pi} \epsilon_0 k}{9e^2} \frac{T}{Nr^2} = 7.503 \times 10^3 \frac{T}{Nr^2} \text{ (MKS)}$
r	general radius or radius of dumbbell hemisphere = 7.76 cm
T_e	electron temperature
T_p	positive ion temperature

LIST OF SYMBOLS (Concluded)

v	ratio of random particle velocity to characteristic velocity
V	across-the-sheath potential
w	probe velocity
α	transcendental function of a/r [see Eq. (1), Appendix V]
δV	potential difference applied between hemispheres
Δ	Laplacian
ϵ_0	dielectric constant = $8.854 \cdot 10^{-12}$ farads/meter
θ	orientation of hemisphere (Figures 9,16)
λ	ratio of probe velocity to characteristic velocity [Eq. (3.4)]
Λ	velocity factor of hemisphere current equations
ρ	charge density

1.0 INTRODUCTION

In the investigation of newly attainable regions of physical interest, it is natural to adopt measuring tools and techniques which have proved useful in earlier, similar studies. Thus, when V-2 rockets became available to scientists after World War II, several University of Michigan investigators suggested and directed the application of Langmuir probes, commonly used in gaseous conduction studies, to ionosphere research.¹⁻³ Each of three of these rockets carried, among many other experiments, an unsymmetrical bipolar probe. The collector geometry, dictated by practical considerations of space and compatibility with other experiments, was less than ideal; however, enough information was obtained to indicate that the technique, more carefully implemented, might prove to be a valuable tool in ionosphere research. Later, when smaller research rockets capable of reaching the ionosphere were developed, this laboratory, with the support of AFCRC, BRL, and later NASA,* renewed its ionosphere research effort.^{4,5} The rather unusual concept of an ejectable Langmuir probe, containing its own current detection and telemetry system, was implemented to insure that: (a) the collector design need not be prejudiced by vehicle imposed limitations, and (b) the probe remain well away from local disturbances of the ionosphere due to outgassing from the burned out rocket motor as well as surface contaminants.

Over the past several years, two different probe configurations have been developed: one, an extremely unsymmetrical bipolar probe to be discussed
*Air Force Cambridge Research Center, Ballistics Research Laboratory, National Aeronautics and Space Administration.

elsewhere, and the other, a dumbbell-shaped, symmetrical, bipolar probe discussed in this report. Earlier works by Boggess,^{6,7} who first discussed the theoretical aspects of the Dumbbell probe, neglected the effects of probe motion. This report includes the effects of probe motion upon the volt-ampere characteristics of the Dumbbell as well as many of the concepts of the earlier treatment.

1.1 GENERAL REMARKS CONCERNING THE DESIGN OF AN EJECTABLE BIPOLAR PROBE

The equations for the ion and electron currents to stationary collectors of planar, cylindrical, and spherical geometries have been known for many years.^{2,7-9} These can be applied to predict, with fair accuracy, the volt-ampere characteristic of any one of the wide variety of bipolar probes which could be formed from various combinations of the above geometries and degrees of symmetry in the respective collector areas.

Although it is the special purpose of this report to consider the theoretical aspects of a particular ionosphere probe, known as the "Dumbbell," it may be useful to discuss briefly some of the factors which guide an experimenter in his choice of the collectors which will form a probe most nearly satisfying the needs and limitations which face him. These factors fall into the following three categories: theoretical considerations, the particular ionospheric parameter to be measured, and available rocket vehicles.

1.1.1 Theoretical Considerations.—It was shown by Hok² and Boggess⁷ that simple asymptotic or approximate solutions to the general current equations are valid, under typical ionospheric conditions, when the collector dimensions are made larger or smaller than certain well-defined limits which

are a function of the temperature and density of the plasma and the collector radius. When the collector is made smaller than the lower limit (typically one or two millimeters), the ion current is said to be orbital-motion-limited. When the collector is made larger than the upper limit (typically several centimeters), the ion current is said to be sheath-area-limited. To take advantage of these mathematically simpler expressions in the predictions of volt-ampere characteristics and in the reductions of ion density data from experimental curves, the collector dimensions may be chosen so that it operates clearly in one mode or the other. In practice, the need for instrumentation space within the probe requires that at least one collector be so large that it necessarily operates in the sheath-area-limited mode, while the other collector may be dimensioned to operate in either of the limiting modes. Thus apparently the probes most easily handled theoretically will be symmetrical, or nearly so (both collectors sheath-area-limited), or greatly unsymmetrical (one collector operating in each mode).

1.1.2 The Particular Ionospheric Parameter to be Measured.—In general, the volt-ampere characteristics of either the symmetrical or the unsymmetrical form of probe do not lend themselves equally well to the determination of all the ionospheric parameters which electrostatic probes are capable of measuring. The symmetrical probe, for example, is not well suited to electron density measurements since the collectors of this type of probe operate in a voltage region where the electron current is a rapidly varying function of collector potential, which can be determined only with limited accuracy. However, the small collector of a greatly unsymmetrical probe can be forced to operate

at any potential and, when driven to the plasma potential, collects just the random electron current from which the electron density is readily obtained.

The electron temperature is based upon the measurement of the electron energy distribution, any part of which is sufficient for the determination of temperature, if a Maxwellian energy distribution is known to exist. Either type of probe is suitable for this measurement; however, the symmetrical probe has access only to those electrons having energies exceeding the negative potential of the collectors, and thus can measure only the high-energy end of the distribution. If the distribution is not purely Maxwellian, this presents a possibility of an incorrect temperature determination, if indeed the term "temperature" can be used to describe such a distribution. The smaller collector of an unsymmetrical probe, however, can be driven through a wide range of potential and therefore can sample the entire electron population. This enables one to obtain a better measurement of the thermal energy. There is, however, evidence^{10,11} that a collector which is near, or above, the plasma potential introduces more disturbance to the plasma than does the symmetrical probe. Thus the choice of probe best suited for this purpose is a question which requires further study.*

The positive ion density may be obtained with either the symmetrical or unsymmetrical probe, although the former appears to offer the most

*A combination symmetrical and unsymmetrical probe, a modified Dumbbell, was launched at Wallop Island, Virginia, in March, 1961, and the temperatures from both types of probes are being compared.

straight-forward measurement. The ion density is based on the measurement of ion current to a collector which is a function of the charged particle density, mass, and temperature as well as the "effective" area of the collector. The effective area of the collector for ions is somewhat greater than its surface area, because of the positive ion sheath which surrounds it. Since the calculation of the effect of the sheath is based on several assumptions and approximations, it is expedient to select a collector which is much larger than the sheath dimensions so that the ion current dependence upon the sheath is kept small. One could, of course, use the unsymmetrical probe for ion density measurements if the ion current equations describe the current collection with sufficient accuracy.*

1.1.3 Rocket Vehicle Considerations.—Ideally, to insure sheath-area-limited operation of the large electrode over a greater range of ion densities, one would like to maximize the dimensions of at least one electrode. However, until recently the only available research rockets with adequate peak altitude capability were of small diameter. This has limited the size of the largest collector to roughly the diameter of such rockets, 6 to 8 inches. If the rocket itself acts as one collector of the bipolar probe, this problem is somewhat reduced since the surface area of the rocket is usually adequate. However, several other problems arise when the rocket is made part of a probe system, aside from the possible contaminating effect of the vehicle. Probably the most important of these problems is the changing

*The modified Dumbbell probe mentioned in the previous footnote is well suited to the evaluation of the measurement of ion density by the two types of probes.

equilibrium potential of the rocket as it changes orientation (tumbles and spins) in free fall. Since the rocket acts as a reference element for application of a potential to the smaller collector, its changing potential enters as an unknown variable in the volt-ampere curves of the probe system. The error due to this can be minimized, however, by selecting a sweep voltage rate which is fast compared to the changes in rocket orientation.

1.2 SELECTION OF THE DUMBBELL FORM OF PROBE

The selection of the Dumbbell configuration was made on the basis of several of the design considerations outlined in the previous section. Theoretical considerations indicated that a symmetrical probe could be expected to introduce less disturbance in the surrounding plasma,^{10,11} since such a probe causes less electron depletion of the plasma than does an unsymmetrical probe. To provide adequate instrumentation space within the electrodes of the ejected probe, both collectors of the symmetrical pair were necessarily sheath-area-limited.

Collectors having spherical geometry were chosen over cylindrical or planar collectors primarily because of the effectiveness with which spherical collectors can be guarded to reduce the electrostatic fringe effects. In general, guard systems for cylindrical and planar collectors are larger, more elaborate, and less effective. For example, a cylindrical collector, having two ends, requires two guard electrodes both of which are insulated and driven at the same potential as the collector. The planar electrode requires a planar guard having minimum dimensions of several sheath thicknesses

which would cause it to be considerably larger than the collector itself. A second advantage of the spherical collector is its nearly linear ion saturation region which simplifies the task of electron temperature reduction by the log plot technique to be discussed.

The availability of the 6-in. diameter Nike-Cajun combination and 8-in. Aerobee 300 or "Sparrobee" indicated that a probe instrument having 6-in. electrodes would be the largest which could be employed with the then existing high-altitude vehicles. This seemingly small size presented no problem, however, since calculations showed that a hemisphere of this size would be large enough to operate within the sheath-area-limited mode in a plasma having electron and ion densities as low as $10^4/\text{cc}$. This would make the results valid to well over 1000 km at which altitude the electron density is typically $10^5/\text{cc}$. Although the separation between the Dumbbell hemispherical collectors was determined by the requirement that the entire probe act as a half-wave dipole antenna at the telemetry frequency, a certain minimum spacing between the collectors was required to prevent the sheath of one end from overlapping that of the other. Calculations show that the sheaths do not begin to overlap until the density falls to approximately $10^4/\text{cc}$, again well over 1000 km.

Thus the Dumbbell, a double-sphere, sheath-area-limited, symmetrical probe, took form as a first attempt at an electrostatic ionosphere probe which would (a) introduce a minimum of disturbance to the surrounding plasma, (b) produce volt-ampere curves most easily interpretable, and (c) be small enough to be carried to great altitudes in the then available vehicles.

1.3 THE DUMBBELL PROBE INSTRUMENT

Figures 1 and 2 are photographs of an assembled and partially disassembled Dumbbell probe, and Figure 3 is a functional block diagram of the system.

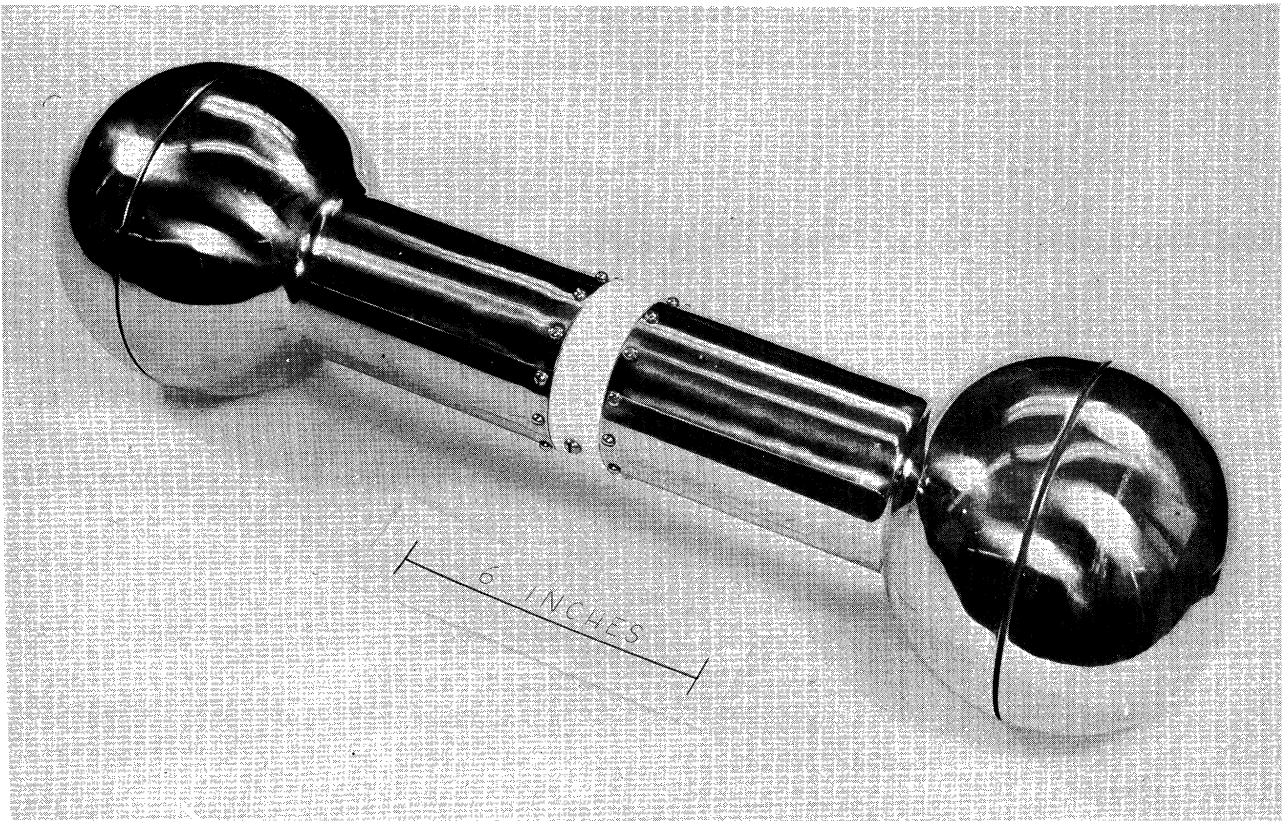


Figure 1. The Dumbbell instrument.

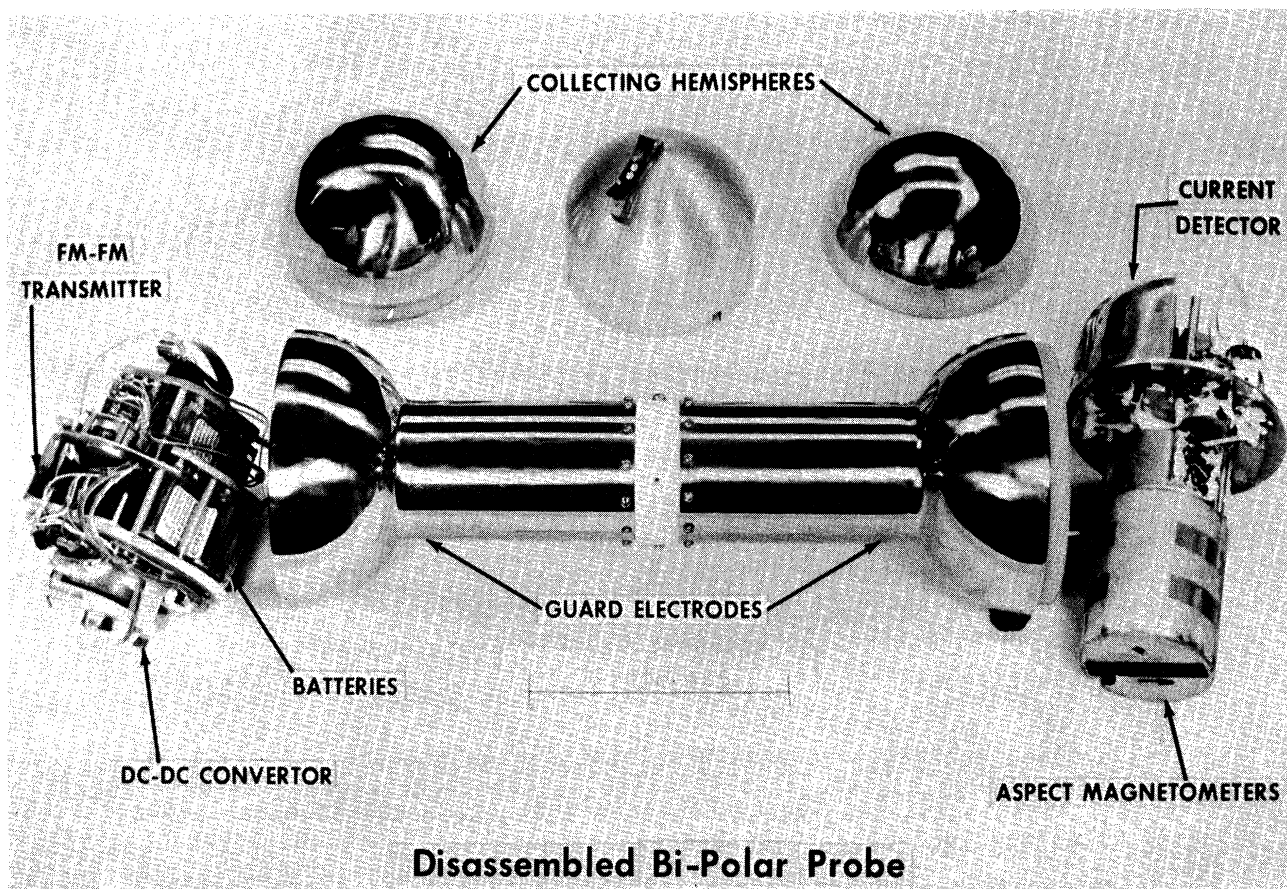


Figure 2. Partially disassembled Dumbbell.

The external structure consists of two stainless-steel hemispherical collectors and two somewhat funnel-shaped guard electrodes which are insulated from the collectors and from each other.

Two identical, sawtooth voltages (δV), are applied between the hemispheres and between the guard electrodes. Two current detectors are connected in series with the hemispheres and the associated δV generator and, since this system is insulated from the "funnel" circuit, measure only the net current flowing to a hemisphere from the plasma. The detectors have 1- μ a and 4- μ a full-scale sensitivities, respectively, which together enable adequate resolution in the measurement of probe currents generally encountered throughout the various regions of the ionosphere. In-flight calibration of the current measurement system is accomplished by substitution of a known resistance for the "ionosphere" periodically during flight.

Also contained within the Dumbbell is an FM-FM telemetry system consisting of a two-watt Bendix TXV-13 transmitter and three voltage-controlled oscillators, providing three information channels: one for each current detector and a third, time-shared by magnetic aspect sensors and other auxiliary circuits used to convey various operational information. Completing the telemetry system is the antenna which consists of the entire external surface of the Dumbbell (very wide band) acting as a half-wave dipole at 220 mc.

The current measuring and telemetry systems have a common power supply, employing a d-c to d-c converter operating from a 24-v pack of HR-1 Silver-Cadmium cells. The instrument and its electronic components are discussed in more detail in other reports.^{5,7,12}

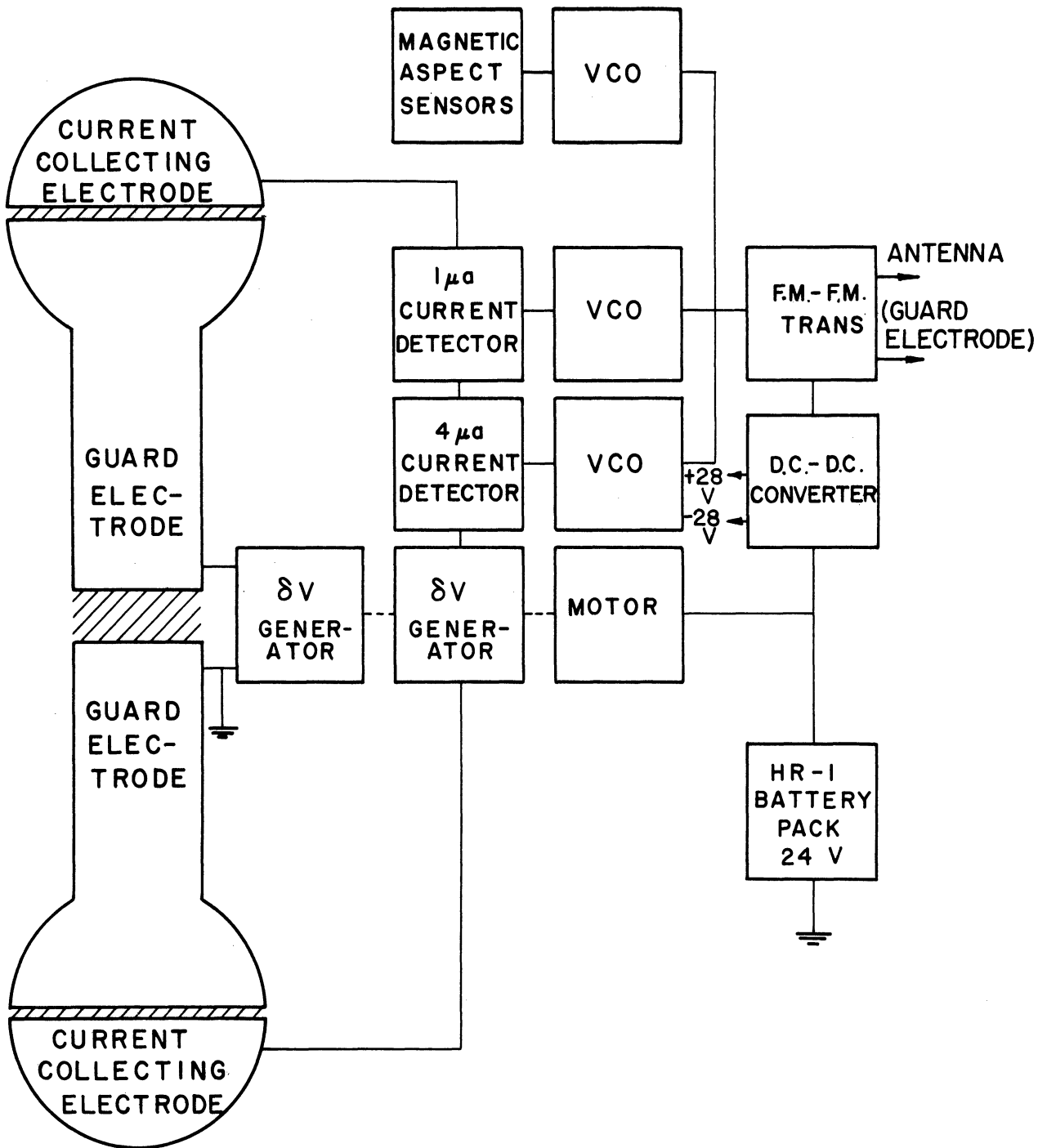


Figure 3. Functional block diagram showing bipolar probe system.

In use, the instrument is carried by a suitable rocket to the lower edge of the ionosphere (approximately 75 km) where a mechanical timer initiates ejection from the rocket by spring action as depicted in an artist's conception reproduced as Figure 4. The rocket and instrument, with increasing separation, follow an elliptical path in free fall to a peak altitude of several hundred kilometers (depending upon the vehicle); their position and velocity is observed by a DOVAP or a RADAR system or both. Throughout the flight, volt-ampere curves of the Dumbbell, immersed in the ionosphere, are continuously measured and transmitted to one or more ground stations where they are recorded. Each curve is later available for interpretation in terms of the electron temperature and positive ion density of the plasma which surrounded the probe at the time of recording.

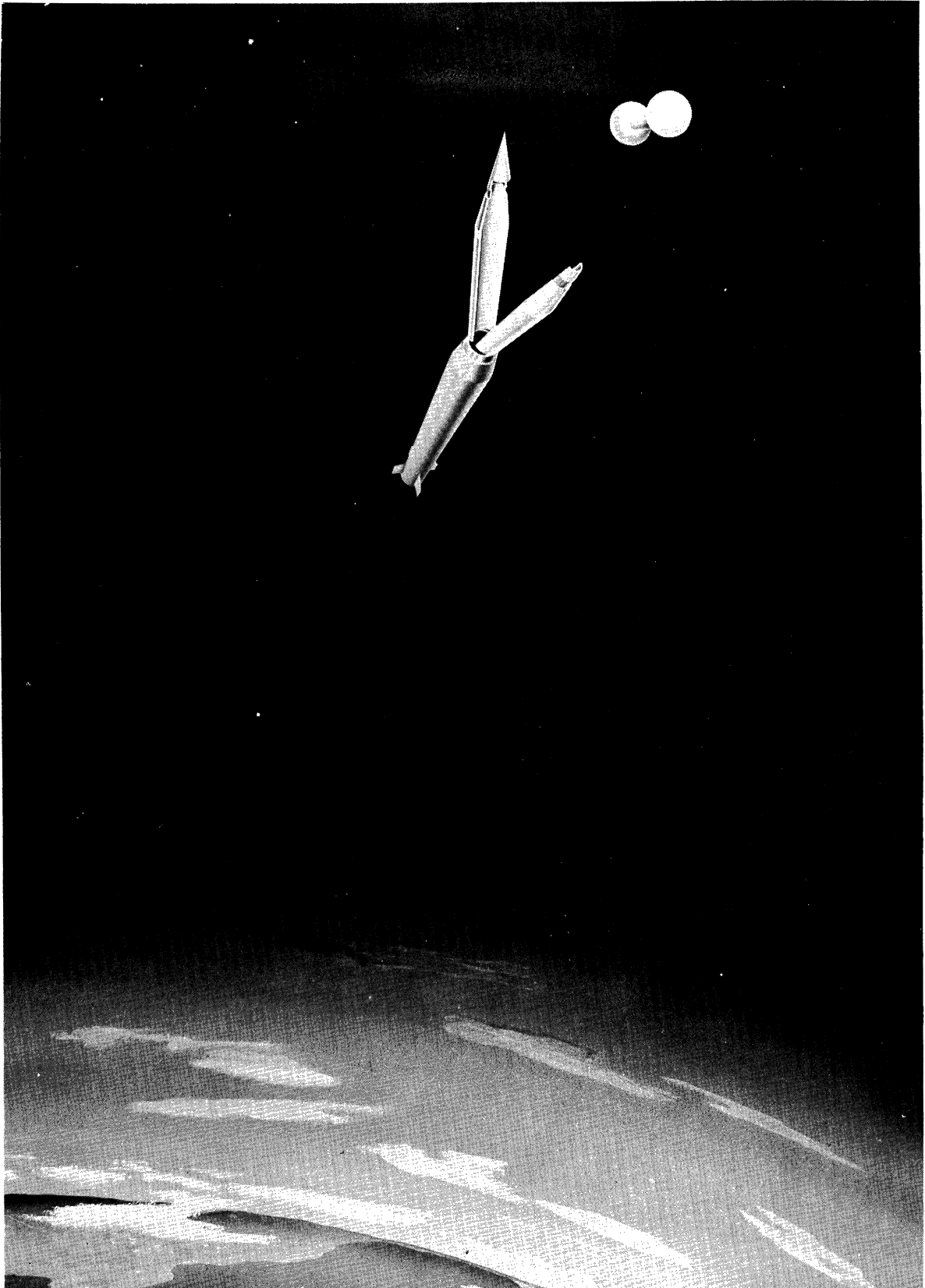


Figure 4. Artist's conception of the ejection of the dumbbell into the ionosphere.

2.0 GENERAL DISCUSSION AND PHYSICAL ASSUMPTIONS

2.1 PHYSICAL ASSUMPTIONS CONCERNING THE EARTH'S IONOSPHERE

The region under investigation by the Dumbbell probe technique extends from approximately 100 to 1000 kilometers. In addition to the neutral particles, it contains a charged particle population consisting of electrons and positive ions in nearly equal numbers. The ion mass number varies continuously from a value of 30 (predominantly NO^+) at lower altitudes to 16 (predominantly O^+) at intermediate altitudes and somewhat lower at higher altitudes where the H^+ and He^+ components become important.¹³ The particle velocity distribution is Maxwellian, at least within each species. However, the ion, electron, and neutral particles are not necessarily in thermal equilibrium with each other, that is, the electron temperature cannot be assumed equal to the ion (and gas) temperatures. Such inequality of temperatures is observed in laboratory gaseous conduction studies where the electron temperature greatly exceeds the gas temperature, and has been postulated^{14,15} and demonstrated¹⁶ for the daytime ionosphere. Such a nonequilibrium condition is possible when energy is imparted to the charged particles selectively and the energy-loss mechanisms are inefficient or selective.

2.2 THE POSITIVE ION SHEATH

Consider now a metallic probe, such as one of the Dumbbell hemispheres, inserted into the ionospheric plasma. Initially, the flow of charge to the surface due to thermal motion is predominantly negative because of the higher

velocity of the electrons. Thus the probe acquires a negative surface charge. To neutralize this surface charge, the plasma surrounds the collector with an ion sheath, a region of net positive charge, so that the probe and sheath combination has zero net charge. The collector comes to an equilibrium potential, V_W , which causes zero net current to flow. An electron or ion moving outside the sheath experiences no electric field due to the probe. Charged particles entering the sheath experience an accelerating force: electrons are retarded and positive ions are attracted. Since the random motion of the particles is undisturbed outside the sheath, one can consider that the particles are emitted toward the collector from the sheath edge with a Maxwellian velocity distribution. If the probe is moving relative to the plasma, then the velocity at the sheath edge is the sum of its random velocity and the relative drift velocity. Because the sheath edge is considered an emitter of particles, it is necessary in computing the emitted current to have some knowledge of its location with respect to the probe surface. Determining the location of the sheath edge is difficult since no sharp boundary between sheath and undisturbed plasma exists. However, in calculating the current to the probe, one must assume that the transition takes place over a zero distance so that the particles may be said to emerge from a well-defined sheath edge. For simplicity the sheath about the hemispherical collector is considered to be spherical so that the electric field is radial. It follows (assuming no collisions) that a particle in moving from some point outside, or at, the sheath edge to some point inside the sheath is affected only by the difference in potential between the sheath edge and the internal point.

2.3 THE EFFECTS OF PROBE MOTION

The positive ion current to a stationary collector is based on two considerations: (1) the Maxwellian velocity distribution of the randomly moving particles; (2) the existence of the sheath which extends the probe's influence beyond its surface. The magnitude of the sheath effect on the ion current depends primarily on the size of the collector in relation to the thickness of the sheath surrounding it. For example, the current to a very large collector (say of an extent greater than one meter) is due almost exclusively to the random motion of particles striking its surface, and the relatively small sheath (having a thickness of a few centimeters) does not significantly contribute to the current. Conversely, the ion current to a very small collector is greatly affected by sheath considerations (sheath size and potential).

When evaluating the ion current to a collector moving relative to the plasma, such as a rocket-borne probe, one must consider the effect of the motion on: (1) the velocity distribution of the ions relative to the collector, and (2) the shape of the sheath and the potential in the sheath. Normally the shape of the sheath is assumed to be the same as that of the collector, but motion of the collector causes the sheath to compress in front and trail out behind.¹⁵ The calculation of the random current to an arbitrarily shaped surface using the Maxwellian distribution with a superimposed drift velocity is in principle straight-forward. However, the distortion of the sheath due to the probe motion, and the resulting modifications in the current which this brings about, is very difficult to calculate.

As indicated above, if the collector is large, the influence of the sheath on the current is small, so that the velocity-induced distortion of the sheath will cause a negligible change in the ion current. However, when the collector is small, the distortion of the sheath is considerable, and one is faced here with the difficult problem of determining the new shape before the ion current can be calculated.

Returning to the problem at hand, the collectors of the Dumbbell probe fall somewhere between the two extremes considered above, but are somewhat closer to the former case. Thus, even though the sheath distortion due to probe motion may vary as much as 50% over the range of velocities encountered by the Dumbbell probe, the net effect of the sheath distortion upon the positive ion current is estimated to be less than 10%. In view of its relatively small effect and the difficulty involved in treating it, the sheath distortion problem is not considered in this report. However, the derivations in this report do include the more important effect due to the modification of the Maxwellian distribution by the drift velocity.

2.4 THE MEAN FREE PATH OF THE IONS AND ELECTRONS

The mean free path is assumed large compared to the dimensions of the sheath, so that essentially no collisions between particles occur within the sheath, and particle trajectory considerations can be used in the development of the current equations. Although this is no longer true below 100 km, it is quite valid for the region above 100 km in which the Dumbbell probe is used.

2.5 THE EFFECT OF THE EARTH'S MAGNETIC FIELD

The geomagnetic field influences the collection of current to a moving

collector in two ways: by altering (1) the charged particle trajectories, and (2) the collector potential. The field causes the particles to follow spiral paths with an average radius of gyration which is larger than the thickness of the sheath. Thus the individual particle trajectories are essentially unaltered by the magnetic field while in the sheath. Then, to a close approximation, the particle trajectories are altered only by the sheath's electric field. The second effect concerns the potential induced in the collector due to its motion through the field. Calculation shows that the potential induced across a Dumbbell hemisphere is on the order of a few millivolts (at typical rocket velocities). Since the hemispheres normally operate in the range of one to four volts with respect to the plasma, the induced potential is considered negligible.

2.6 PHOTOEMISSION DUE TO SOLAR RADIATION

The mechanism of photoemission is well understood and one can make reasonably accurate calculations of the current to be expected when the incident radiation and the work function of the target are known. However, for a probe traveling through the ionosphere, both of these factors are uncertain. The photon flux spectrum is not a well-defined function of altitude and is certainly subject to wide diurnal and seasonal variations. The work function of the collector surfaces is strongly affected by the surface conditions of the metal, which, though carefully cleaned before flight, can absorb gas particles during the flight. In view of these uncertainties in the calculation of photoemission, the authors have relied on rocket-borne measurements when considering its effect upon the Dumbbell probe results. On the basis of Hinterreger's¹⁷ measurements of photocurrent from a rocket-borne tungsten collector, it is estimated that the photoemission from a

Dumbbell collector is small compared to the ambient ion current densities at least up to 1000 km. Since the particle mean free path is long compared to the sheath thickness, the photo-electrons leaving the collector surfaces have no direct interaction with the incoming positive ions and electrons. They do, however, constitute a net positive current to the probe and thus, if not corrected for, produce a small error in the ion density determinations at higher altitudes where the photocurrent may not be considered negligible.

It is appropriate here, before deriving the current equations, to review the assumptions, presented above, on which the hemisphere current equations are based. The negatively charged hemisphere is surrounded by a spherical positive ion sheath which is permeated by a radial electric field terminating at the sheath edge beyond which the velocity distribution of electrons and ions is Maxwellian. Inside the sheath, the electrons and ions do not interact, but move according to their initial velocities and the velocity they acquire from the local electric field. The probe moves through the plasma with a low relative drift velocity which does not alter the spherical symmetry of the sheath but serves only to modify the Maxwellian velocity distribution relative to the collector.

3.0 DERIVATION OF THE MOVING-HEMISPHERE CURRENT EQUATIONS

3.1 RANDOM POSITIVE ION CURRENT TO A DUMBELL HEMISPHERE

The positive ion current to a hemisphere is equal to the random positive ion current to the sheath edge since the dimension of the collector and the ion number density and temperature insure that almost all positive ions which cross the sheath edge are intercepted by the collector.⁷ The derivation of the random ion current to the sheath surface follows. It can be shown that the current density to an infinitesimal surface element oriented with its normal along the x axis and moving relative to the plasma with a normal velocity λ_x , is given by

$$j_x = \frac{N_p e c_p}{\pi^{3/2}} \iiint (v_x + \lambda_x) \exp(-v^2) dv_x dv_y dv_z \quad (3.1)$$

where the integration limits are found from the condition that the particles can have any tangential velocity (v_y and v_z) and only a positive normal velocity relative to the area element.

$$0 < v_x + \lambda_x < \infty, \quad -\infty < v_y, v_z < +\infty \quad (3.2)$$

N_p is the particle number density, c_p is the particle characteristic velocity expressed in terms of the particle mass and temperature as given by

$$c_p = \sqrt{\frac{2kT_p}{m_p}}, \quad (3.3)$$

v is the ratio of Maxwellian particle velocity to the characteristic velocity, and λ is the collector drift velocity, w , divided by the characteristic velocity, c . From the definitions,

$$\lambda_p = \frac{w}{c_p} = w \sqrt{\frac{m_p}{2kT_p}} \quad (3.4)$$

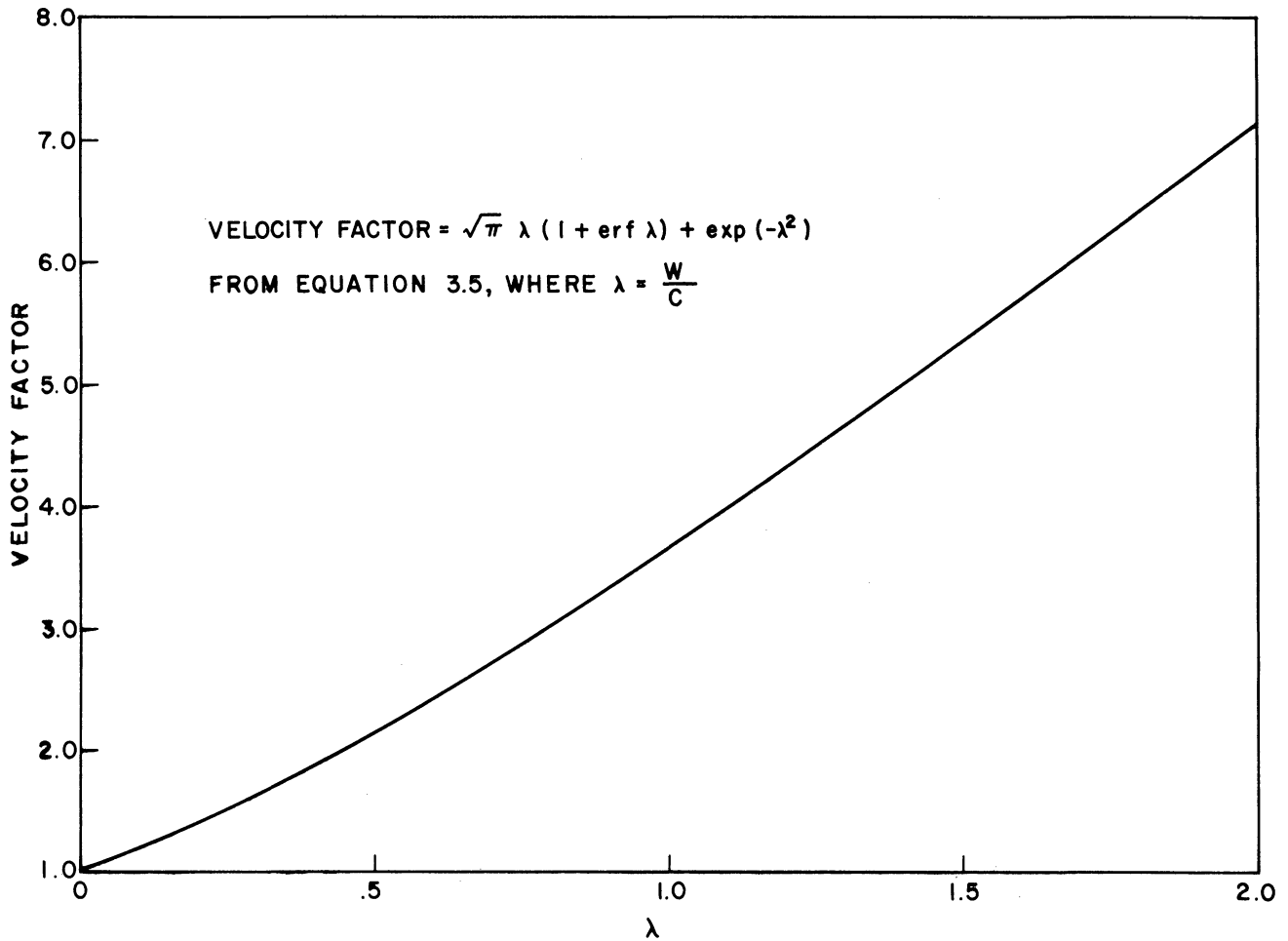


Figure 5. Velocity factor of the random current density.

Having found the current density to an area element at the sheath hemisphere, it is now necessary to integrate (3.5) over the hemisphere to obtain the ion current. The integration of Eq. (3.5) is carried out in Appendix II. The resulting random ion current to a hemisphere is given by

$$i_p = \frac{N_p e c_p}{2 \sqrt{\pi}} 2 \pi a^2 \Lambda(\lambda, \theta) \quad (3.7)$$

The function $\Lambda(\lambda, \theta)$, representing the contribution to the current due to the drift motion, is given by

$$\Lambda(\lambda, \theta) = \frac{\sqrt{\pi}}{2} \left(\lambda + \frac{1}{2\lambda} \right) \operatorname{erf} \lambda + \frac{1}{2} \exp(-\lambda^2) + \frac{\sqrt{\pi}}{2} \lambda \cos \theta \quad (3.8)$$

where θ defines the hemisphere orientation (see Figure 16).

In (3.7) the quantity $2\pi a^2$ represents the area of the sheath about the hemisphere. When the drift velocity approaches zero, the limiting value of the velocity factor approaches unity and (3.7) reduces to the random current to a stationary hemisphere

$$i_p = \frac{N_p e c_p}{2 \sqrt{\pi}} 2\pi a^2 \quad (3.9)$$

At the other extreme, where the drift velocity increases without limit, the current becomes linear with velocity and also increases without limit.

$$i_p \underset{\lambda \rightarrow \infty}{\simeq} N_p e v \pi a^2 \left(\frac{1 + \cos \theta}{2} \right) \quad (3.10)$$

Note that (3.10) is simply the drift current to the projected area of the hemisphere. The variation of the velocity factor Λ at small drift velocity, λ , and for various orientations, θ , is shown in Figure 6.

3.2 ELECTRON CURRENT TO A DUMBBELL HEMISPHERE

The effect of the rocket velocity upon the electron velocity distribution relative to the collector may be considered negligible even at satellite velocities (0.3% at 8×10^3 m/sec), since, for electrons, λ is nearly zero.* In view of this, the electron current to a hemisphere is given by (see Appendix III for derivation):

$$i_e = \frac{N_e e c_e}{2 \sqrt{\pi}} 2\pi r^2 \exp \left(- \frac{eV}{kT} \right) \quad (3.11)$$

This is simply the random current to the Dumbbell hemisphere area, $2\pi r^2$, modified by the exponential factor arising from the Maxwell-Boltzmann distribution law.

*See Appendix VI for discussion of other factors affecting the electron current.

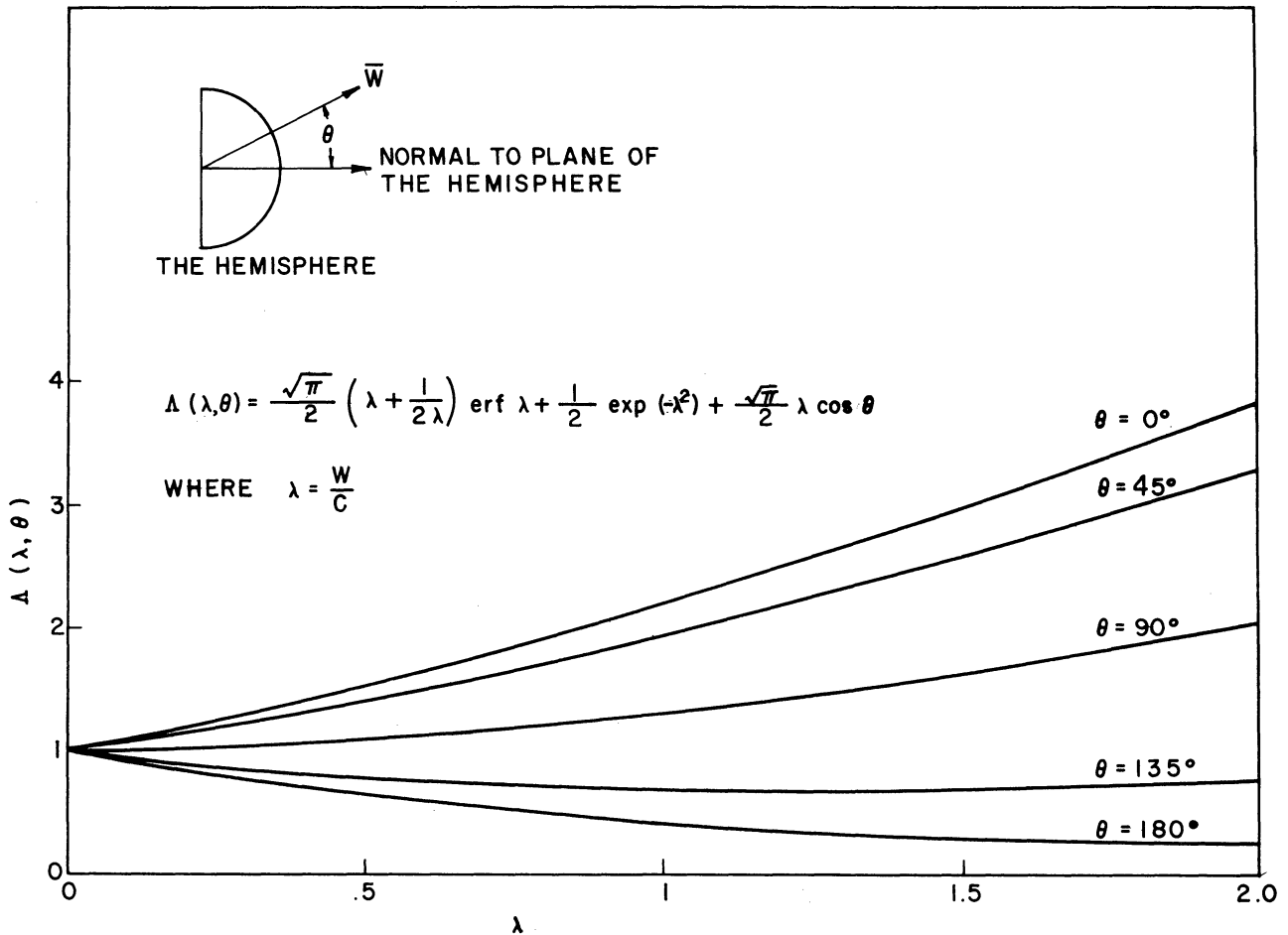


Figure 6. Velocity factor $\Lambda(\lambda, \theta)$ of random hemisphere current.

3.3 THE NET HEMISPHERE CURRENT

The net current to a single hemisphere, (3.12), is the sum of the positive ion current, (3.7), and electron current, (3.11), and any other components such as photo-current and negative ion current which, if present, would be included.

$$i = \frac{N_p e c_p}{2\sqrt{\pi}} 2\pi a^2 \Lambda - \frac{N_e e c_e}{2\sqrt{\pi}} 2\pi r^2 \exp\left(-\frac{eV}{kT}\right) + i_{\text{photo}} - i_{\text{neg}} + \dots \quad (3.12)$$

Rewriting this and excluding the other components, the total current can be written in the form

$$i = \frac{N_p e c_p}{2\sqrt{\pi}} 2\pi r^2 \left[\frac{a^2}{r^2} \Lambda - \frac{N_e c_e}{N_p c_p} \exp\left(-\frac{eV}{kT}\right) \right] \quad (3.13)$$

In a given plasma, only two of the parameters in (3.13) can be considered variables, i.e., the sheath radius, a , and the across-the-sheath potential, V . However, closer inspection reveals that the sheath thickness and the potential

are not independent variables. When the sheath shrinks to the probe surface, the potential must necessarily vanish, and when the sheath grows very large, it is able to support a large potential difference.

The dependence of a upon V can be viewed from another approach. The total charge on the probe determines the radial electric field at its surface, and the electric field integrated over the sheath determines the across-the-sheath potential. Also, the total charge on the probe determines the number of positive charges necessary to preserve charge neutrality which fixes the size of the sheath for a given ion density and temperature in the undisturbed plasma. Thus the dimensions of the sheath and the potential are related by the ionosphere parameters. Such a relationship is found in the next section and is applied to obtain an expression for the net current as a function of V alone.

3.4 THE RELATIONSHIP BETWEEN THE SHEATH RADIUS, a , AND THE ACROSS-THE-SHEATH POTENTIAL, V

A second, independent equation for the ion current to the hemisphere would make it possible to deduce the relation between the sheath radius and potential. Such a relation may be obtained by the use of Poisson's equation which relates the sheath potential to the charge density in the sheath.

$$\Delta V = \rho/\epsilon_0 \quad (3.14)$$

where ϵ_0 is the dielectric constant of free space and the Laplacian, Δ , is a function only of r because of the spherical symmetry of the sheath and the radial electric field. Following the method of solution of Langmuir⁸ (Appendix IV), a second equation (3.15) for the positive ion current is obtained. This describes the dependence of the ion current on both the sheath radius and the

potential.

$$i = \frac{N_p e c_p}{2 \sqrt{\pi}} 2 \pi r^2 \frac{P}{\alpha^2} \left(\frac{eV}{kT_p} \right)^{3/2} \quad (3.15)$$

where

$$P = \frac{8 \sqrt{\pi} \epsilon_0 k T_p}{9 e^2 N_p r^2} \quad (3.16)$$

and α is a transcendental function of (a/r) .

Equation (3.15) states that the current depends on the $3/2$ power of the voltage and on the sheath radius through the function α . The previously obtained positive ion current, (3.7), which was found by integrating over the Maxwellian distribution, also expresses the ion current in terms of the sheath radius. By equating the two expressions for positive ion current, a relation between V and a is obtained.

$$\frac{P}{\Lambda} \left(\frac{eV}{kT_p} \right)^{3/2} = \frac{a^2}{r^2} \alpha^2 \quad (3.17)$$

Equation (3.17) relates the potential to the sheath radius explicitly; however, it would be more convenient to have the inverse relationship since the potential is a factor more directly under the control of the experimenter. This inversion is carried out in Appendix V and leads to the following expression for $(a/r)^2$.

$$\frac{a^2}{r^2} = 1 + 2 \sqrt{\frac{P}{\Lambda}} \left(\frac{eV}{kT_p} \right)^{3/4} + \dots \quad (3.18)$$

Equation (3.18) expresses the relationship between, a , and V , which is seen to satisfy the boundary conditions: (1) the sheath shrinks to the probe radius, r , when V vanishes; (2) the sheath grows indefinitely large when the potential tends toward infinity. However, equating the two expressions

for ion current in (3.17) is not entirely valid as may be observed when (3.17) is rewritten

$$\frac{P}{\alpha^2} \left(\frac{eV}{kT} \right)^{3/2} = \frac{a^2}{r^2} \Lambda . \quad (3.17a)$$

The left side of (3.17a) is the result of a derivation which assumes that ions enter the sheath with zero initial velocity with or without drift velocity. The right side of (3.17a) is the result of a derivation which assumes that ions enter the sheath with Maxwellian velocities plus a superimposed drift velocity, if present. In equating the right and left sides of (3.17a), a contradiction results; however, this does not introduce large errors into the resulting equations. Part of the contradiction can be removed by use of an approximate correction factor⁸ which takes into account the Maxwellian distribution in the left side of (3.17a), but it is not used in this report because the gain in accuracy does not justify the increased complexity. This problem is now being studied by the authors and will be discussed in a later report, at which time the error introduced by the use of (3.17a) will be evaluated quantitatively. Relations similar to (3.17) were used by Hok² and Boggess⁷ in earlier reports which did not consider the motion of the probe.

3.5 FINAL FORM OF THE NET HEMISPHERE CURRENT EQUATION

Using the relationship which has been found between the sheath radius, a , and the across-the-sheath potential, V , the net current to a dumbbell hemisphere can be written as a function of the voltage alone. This is accomplished by inserting relation (3.18) into the net hemisphere current equation, (3.13) which results in

$$i = \frac{N_p e c_p}{2 \sqrt{\pi}} 2 \pi r^2 \left\{ \Lambda + 2 \sqrt{P \Lambda} \left(\frac{eV}{kT_p} \right)^{3/4} - \frac{N_e c_e}{N_p c_p} \exp \left(- \frac{eV}{kT_e} \right) \right\} \quad (3.19)$$

When volume neutrality, ($N_e = N_p$) and thermal equilibrium, ($T_e = T_p = T_g$) are assumed to exist in the plasma, (3.19) reduces to the more familiar form

$$i = \sqrt{\frac{kT}{2 \pi m_p}} N e 2 \pi r^2 \left\{ \Lambda + 2 \sqrt{P \Lambda} \left(\frac{eV}{kT} \right)^{3/4} - \sqrt{\frac{m_p}{m_e}} \exp \left(- \frac{eV}{kT} \right) \right\} \quad (3.20)$$

Where the first two terms in the brackets represent the ion current component to the hemisphere and the last term is the electron current. Figure 7 shows the current characteristic of a single hemisphere at various orientations for a fixed velocity ratio, $\lambda = 1$.

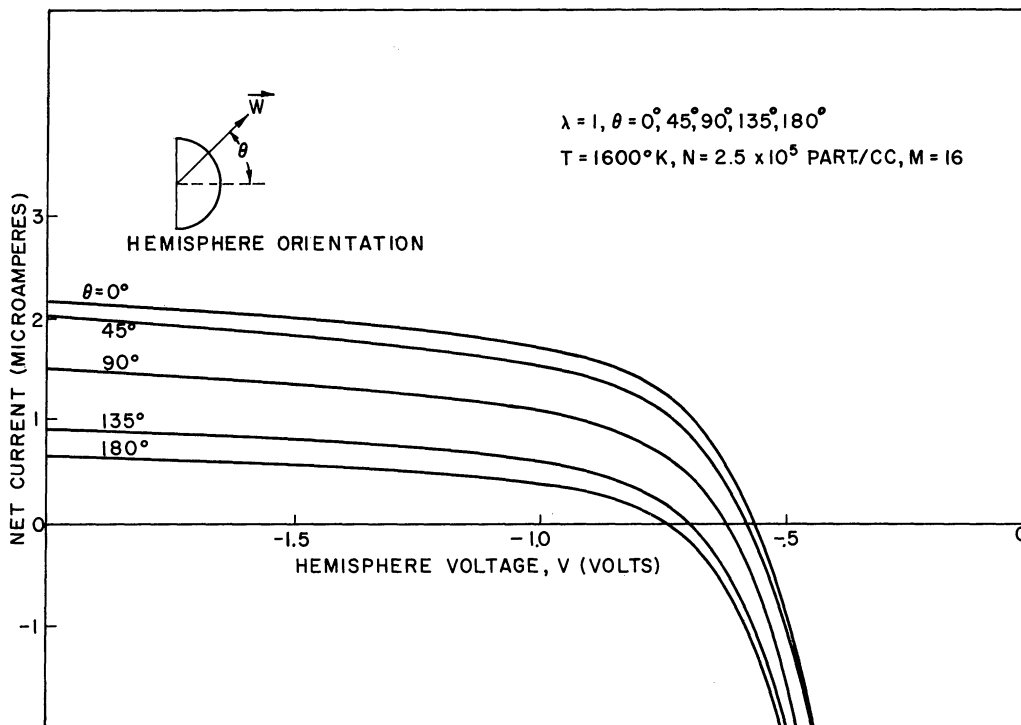


Figure 7. Single-hemisphere current curves for a fixed velocity and selected orientations.

4.0 THE DUMBBELL VOLT-AMPERE CHARACTERISTIC

The Dumbbell collector system consists of two hemispheres, each of which has the current characteristic described by (3.19) or (3.20). Since the net current to the Dumbbell, as a unit in the ionosphere, must be zero, the current to one hemisphere must be equal and opposite to the current to the other, over the entire range of difference voltage which may be applied between them. Using this fact, it is convenient to plot the net current to the individual hemispheres as shown in Figure 8, where one characteristic is inverted and superposed upon the other. Figure 8 shows the superposed currents when one hemisphere is oriented at $\theta = 45^\circ$ while the other is at $\theta = 135^\circ$ as shown in Figure 9.

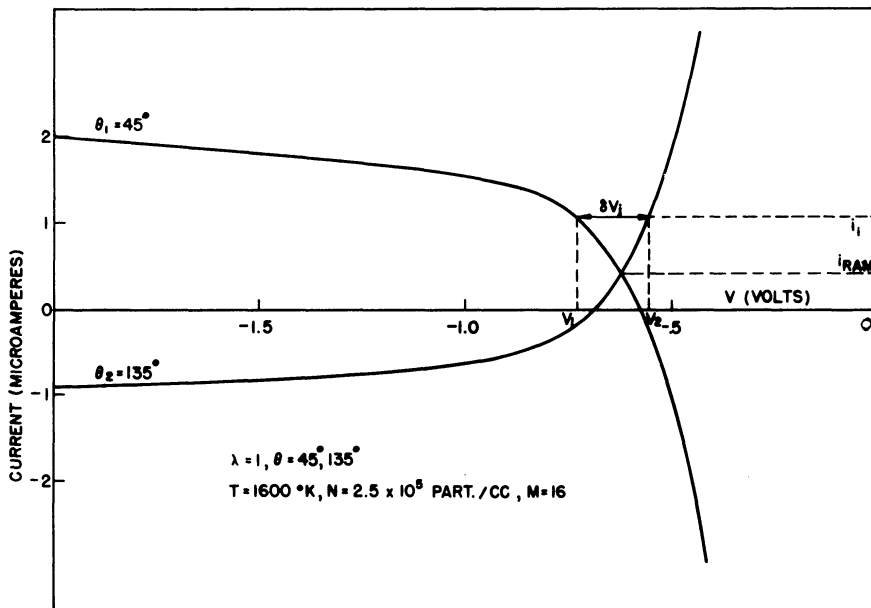


Figure 8. Superposed current characteristics of two oppositely oriented hemispheres.

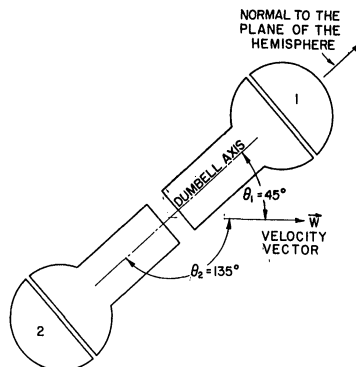


Figure 9. A particular Dumbbell orientation.

The ion current to the leading hemisphere, 1, exceeds that to the trailing hemisphere, 2, so that when the two hemispheres are shorted directly together with no voltage applied between them, a net current, I_{ram} , results. When a particular difference voltage, δV_i , is applied, the hemisphere potentials, V_1 and V_2 adjust to cause a net current i_i , which is just equal to the net positive current to 1 and the net negative current to 2. The volt-ampere characteristic of the pair of hemispheres, at this particular velocity and orientation, obtained graphically by plotting δV versus i , is shown in Figure 10. The right side of the graph is dominated by the current characteristic of hemisphere 1 because the applied voltage occurs mostly as a change

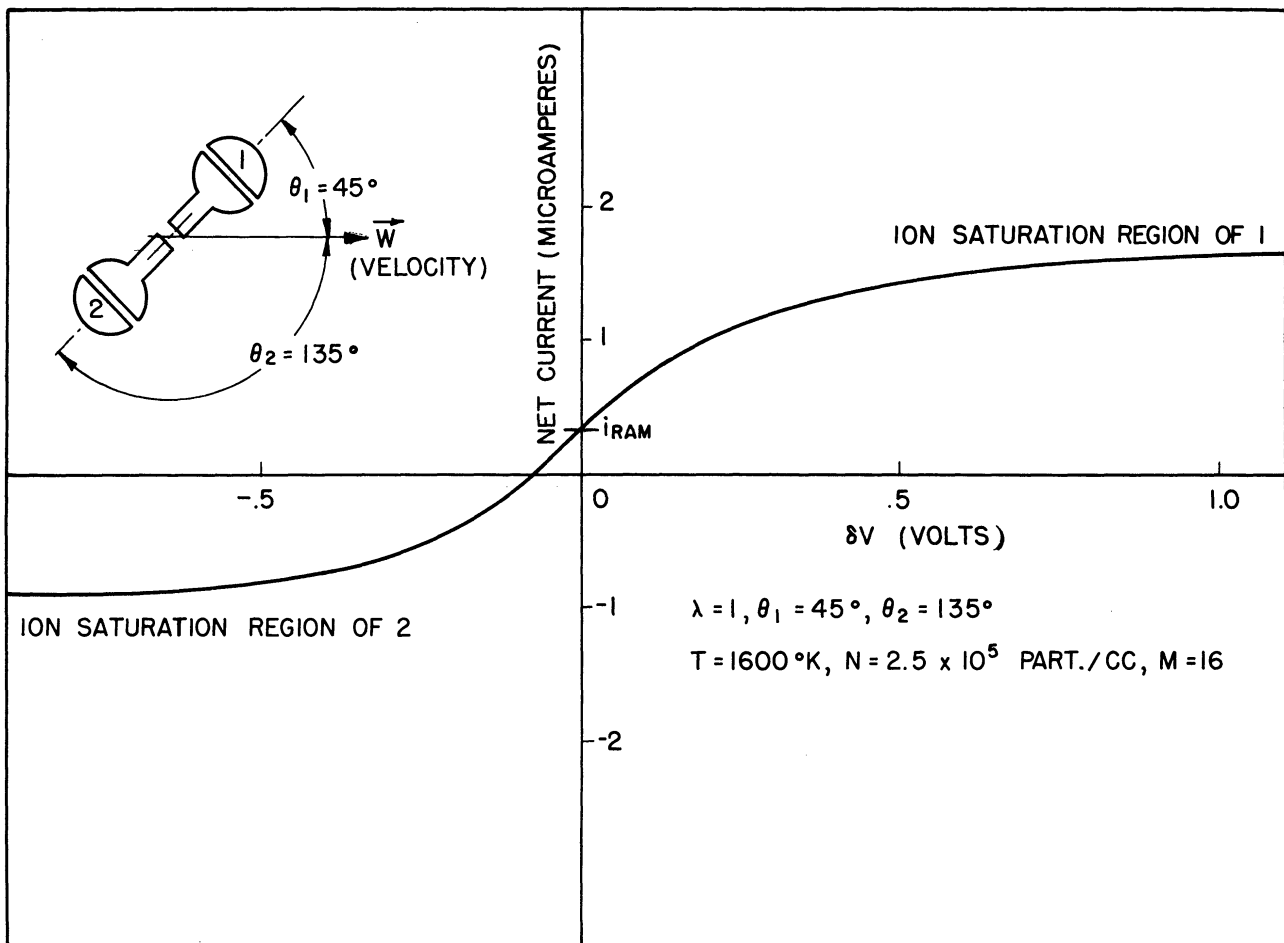


Figure 10. Volt-ampere characteristics of Dumbbell having orientation shown in Figure 9.

in potential at this collector which is being driven negative. The ready availability of electrons prevents the positive-going-hemisphere from accepting much of the δV . This is particularly true at higher values of applied δV as the negative-going-hemisphere approaches the ion saturation region where electrons are completely retarded. Here, the negative-going-hemisphere accepts nearly all the further increase in δV .

Figures 11-14 illustrate the effect of various Dumbbell velocities and orientations upon the volt-ampere characteristics, under typical ionosphere conditions. Figure 11 shows the predicted volt-ampere curves for selected velocity ratios λ when the Dumbbell is oriented so that one hemisphere points forward into the trajectory, $\theta_1 = 0^\circ$, and the other hemisphere points backward along the trajectory, $\theta_2 = 180^\circ$. The right-hand linear portion of each curve represents the ion saturation region of the leading hemisphere, while

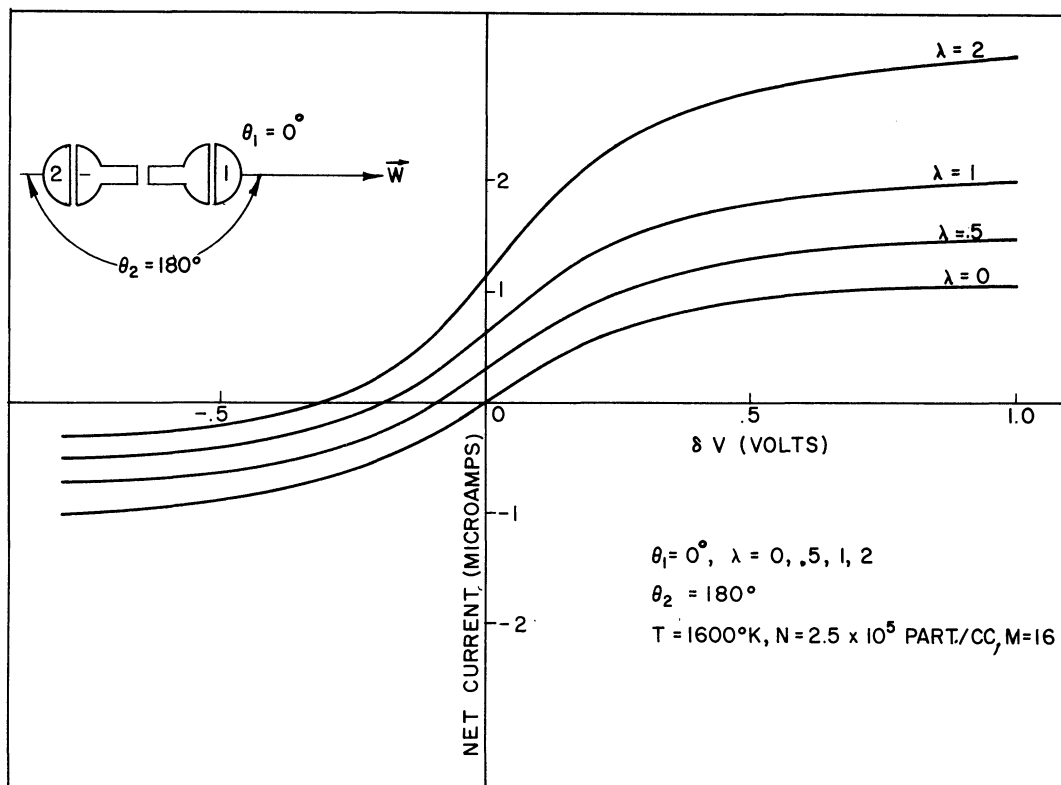


Figure 11. Dumbbell volt-ampere characteristics for $\theta = 0^\circ$ and selected velocity ratios.

the left-hand linear portion represents the same region for the trailing hemisphere. Note that the curve for $\lambda = 0$ represents the stationary probe characteristic and the other curves show the distortion due to various probe velocities. Note further that the leading hemisphere sweeps out more current as the velocity is increased and the trailing hemisphere, leaving the lower velocity ions behind, collects less current. At zero δV , for this orientation, there is a bias current which varies with velocity.

Figure 12 shows the Dumbbell characteristics at the opposite orientation, after the probe has tumbled (rotated) 180° . It is entirely analogous to the previous case except that the leading and trailing hemispheres have switched positions.

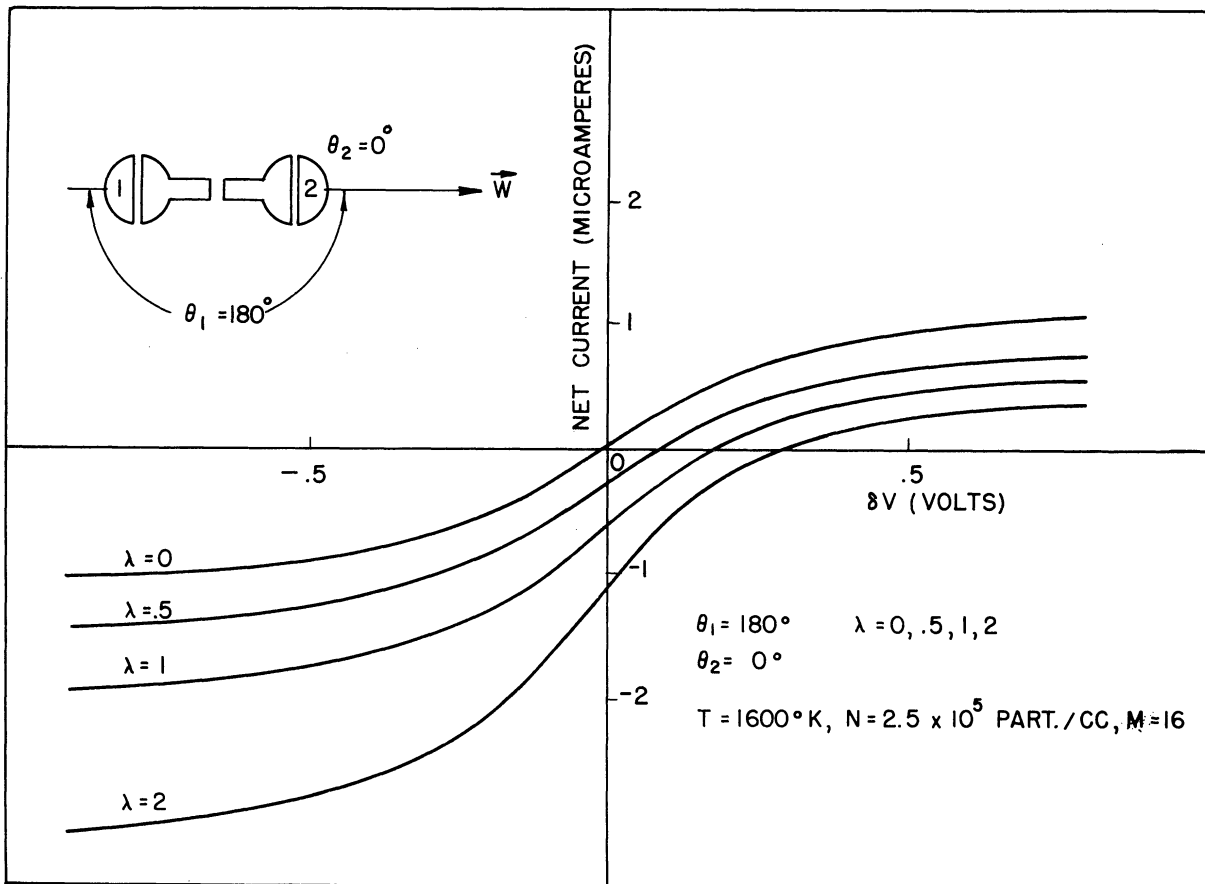


Figure 12. Dumbbell volt-ampere characteristics for $\theta = 180^\circ$ and selected velocity ratios.

Figure 13 shows the characteristics when both hemispheres are perpendicular to the probe velocity, $\theta_1 = \theta_2 = 90^\circ$. As one would expect, the characteristics are symmetrical, and somewhat less affected by velocity than in other orientations. Note that at zero δV , no bias current exists at any velocity since the ion current swept out at each end is identical and therefore cancels.

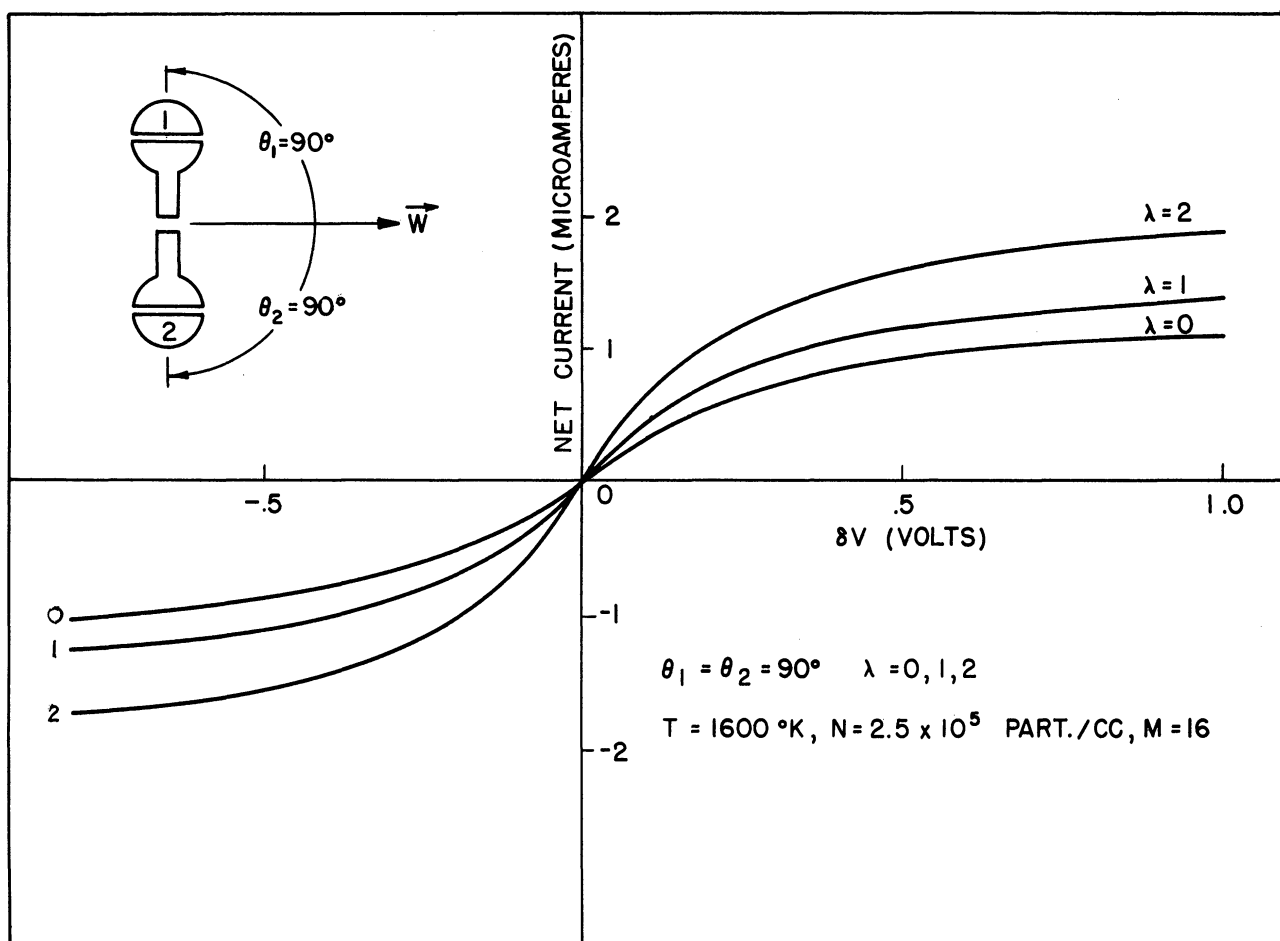


Figure 13. Dumbbell volt-ampere characteristics for $\theta = 90^\circ$ and selected velocity ratios.

Figure 14 shows Dumbbell characteristics at an intermediate orientation in which the trailing hemisphere exhibits a decreasing ion current at lower velocities, and then increases at higher velocities as its small forward-projected area sweeps out greater ion current than is left behind. Similar curves can be drawn for other orientations and velocities, but those shown illustrate the essential features of the Dumbbell characteristics.

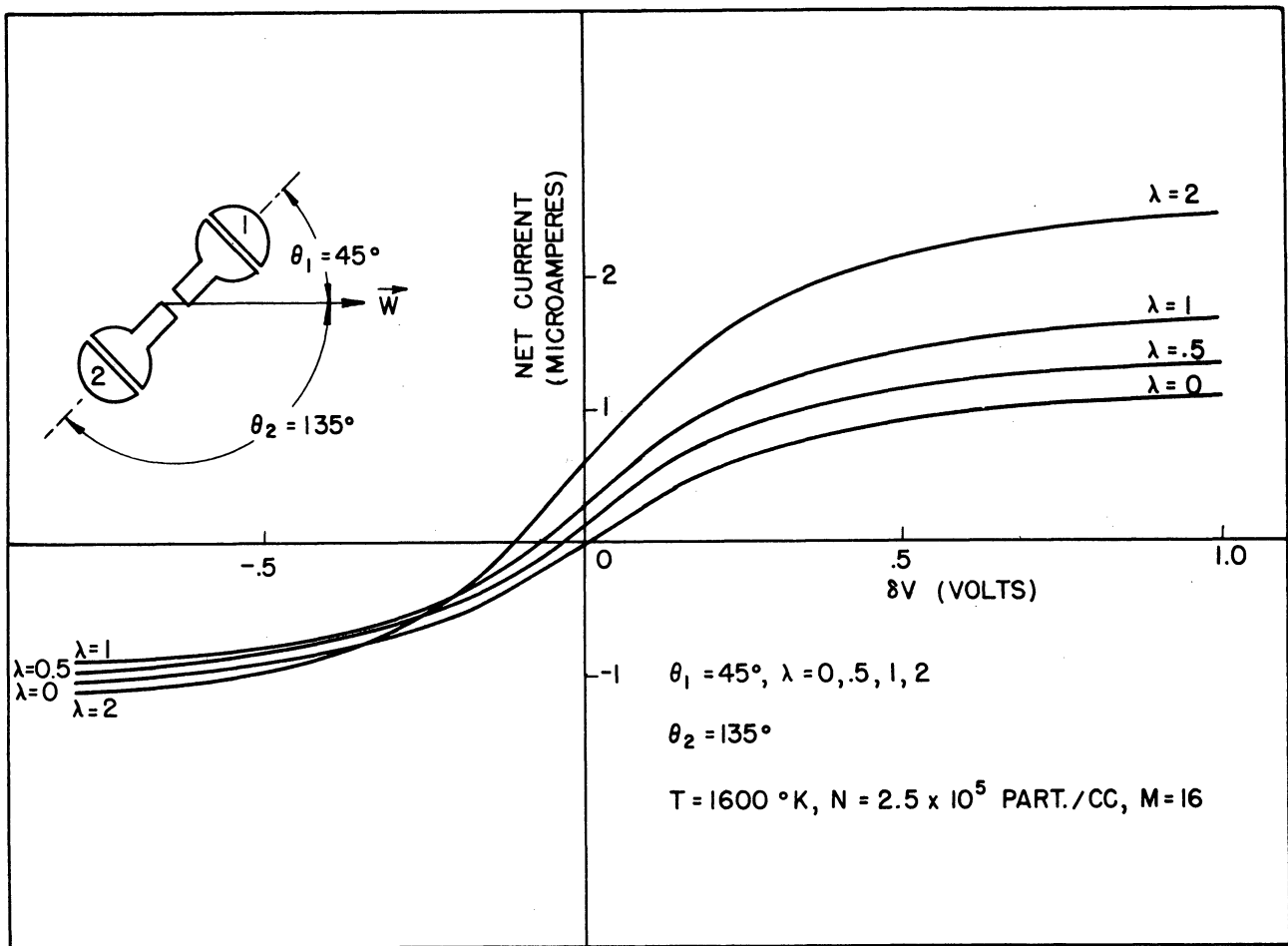


Figure 14. Dumbbell volt-ampere characteristics for $\theta = 45^\circ$ and selected velocity ratios.

5.0 THE METHOD OF ELECTRON TEMPERATURE REDUCTION FROM DUMBELL VOLT-AMPERE CHARACTERISTICS

The determination of electron current from a Dumbbell volt-ampere characteristic is carried out as follows. Since the positive ion saturation region, shown in Figure 15, contains no electron current component (all electrons are retarded), it defines the positive current characteristic of the negative-going-hemisphere. As the applied voltage is reduced, some of the higher-energy electrons overcome the retarding potential and electron current begins to flow, rapidly decreasing the net positive current. The electron current can be separated from the net current by extrapolating the ion current characteristic, as shown in Figure 15, and subtracting the net current from the extrapolated ion current. The extrapolation is straight-forward since the ion current characteristic of a hemisphere is nearly linear with voltage and can be done graphically with a straight edge, or by machine with least-squares fitting.

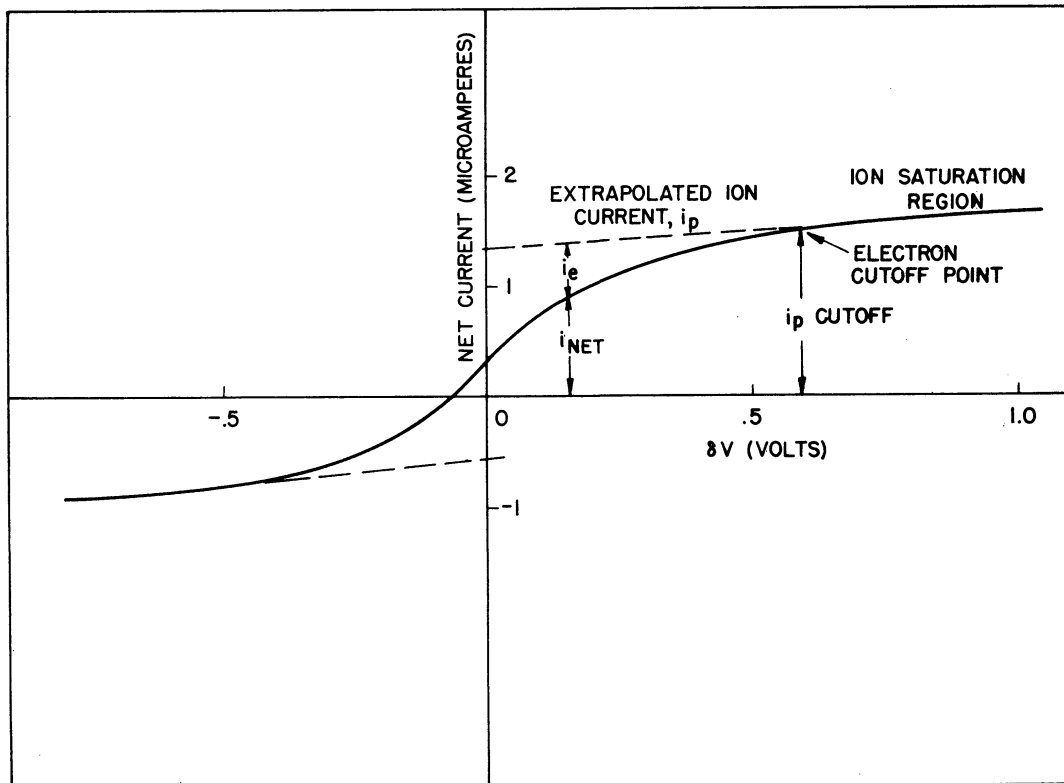


Figure 15. Dumbbell volt-ampere characteristics showing pertinent factors in the reduction of ionospheric parameters.

An important feature of the extrapolation method of obtaining the electron current is that it does not assume that the net positive current is composed only of ion current. It assumes only that the positive current characteristic does not exhibit abrupt changes in character over the relatively small region which is approximated by the extrapolation. Other positive current components such as photoemission due to solar radiation and secondary emission due to high-energy particles are independent of the hemisphere potential and thus will not affect the electron current determination. This method of obtaining the electron current characteristic has the additional feature that the velocity-induced distortion of the current characteristics, in the ion-saturated region, need not be calculated but is actually measured. Thus the extrapolation can be made with confidence, and the effects of velocity will not appear in the electron current characteristic which results.

From the above discussion it can be seen that the electron current characteristic, i_e as a function of δV , can be obtained readily from a theoretical or experimental volt-ampere characteristic of the Dumbbell. Also, it was shown previously that the theoretical relationship between i_e and V is given by (3.11) which is simplified to

$$i_e = K \exp \left(- \frac{eV}{kT_e} \right)$$

where

$$K = \frac{Nec}{2\sqrt{\pi}} 2\pi r^2 \quad (5.1)$$

and, taking the natural log,

$$\ln i_e = \ln K - \frac{eV}{kT_e} \quad (5.2)$$

and the derivative,

$$d \ln i_e = - \frac{e}{kT_e} dV \quad (5.3)$$

which can be rewritten

$$\frac{d \ln i_e}{dV} = - \frac{e}{kT_e} \quad (5.4)$$

If one plots the natural log of i_e versus V on linear graph paper, the result is a straight line of slope e/kT_e and the electron temperature is given by

$$T_e = - \frac{e}{k} \frac{dV}{d \ln i_e} \quad (5.5)$$

Thus, the task of finding the electron temperature, given a volt-ampere characteristic, reduces to that of finding the true change in potential, dV , of the negative-going-hemisphere when the applied δV is known. As discussed in Section 4.0, most of the applied voltage, δV , appears as a change in voltage at the negative-going-hemisphere dV ; so that, to a close approximation

$$dV \approx d\delta V \quad (5.6)$$

However, some change in potential does occur at the positive-going-hemisphere. Theoretical studies using curves such as shown in Figure 8 show that this approximation leads to electron temperature values which are about 10% higher than the true values. That is, in the region of the curve from which the electron temperature is obtained, approximately 90% of the change in δV occurs as a change in potential, dV , of the negative-going-hemisphere, so that, in (5.5), the value of dV can be replaced by 0.9 δV .

6.0 THE METHOD OF REDUCING POSITIVE ION NUMBER DENSITY FROM DUMBELL VOLT-AMPERE CHARACTERISTICS

As stated earlier, the ion current to a Dumbbell hemisphere is just the random ion current crossing the edge of the surrounding sheath. For a sheath radius, a , the ion current is given by

$$i_p = \frac{N_p e c_p}{2 \sqrt{\pi}} 2 \pi a^2 \Lambda(\lambda, \theta) \quad (3.7)$$

where

$$c_p = \sqrt{\frac{2kT_p}{m_p}} \quad (3.3)$$

The sheath radius is given by (3.18), and, neglecting higher-order terms, is the following function of V , θ , T_p , N_p , and m_p .

$$\frac{a^2}{r^2} = 1 + 2 \sqrt{\frac{P}{\Lambda}} \left(\frac{eV}{kT_p} \right)^{3/4} \quad (6.1)$$

Substituting (6.1) into (3.7) and rearranging, the ion current is given by

$$i_p = \frac{N_p e c_p}{2 \sqrt{\pi}} 2 \pi r^2 \left[1 + 2 \sqrt{\frac{P}{\Lambda}} \left(\frac{eV}{kT_p} \right)^{3/4} \right] \Lambda \quad (6.2)$$

where r is the known hemisphere radius. The density appears in (6.2) both as a linear term and as the square root since it is one of the factors in P , [see (3.16)]. Equation (6.2) lends itself well to machine solution for N_p when the other variables i_p and m_p are known. The orientation and velocity factors, θ and λ , are known from trajectory and aspect data. The manner in which they are obtained will be discussed in future reports dealing with the

engineering aspects of the Dumbbell and reports presenting the data resulting from its use. The ion mass, m_p , is assumed on the basis of rocket measurements with Bennett mass spectrometers.^{18,19} Selection of the value of ion temperature to be used in solving (6.2) for N_p is a prerogative of the experimenter. At this time, it is clear that the electron temperature is not equal to the ion temperature in all regions of the ionosphere.^{14,16} However, since the electron temperature is the only directly obtainable temperature by this technique, it appears advisable to assume thermal equilibrium for the present purpose and make corrections later when the amount by which the ion and electron temperatures differ is better defined. Fortunately, the ion temperature enters the density determination only as the square root so that, unless the ion and electron temperatures are greatly different, small error in N_p will result.

The remaining variables, i_p and V , are related by (6.2). Theoretically, one could use the values of i_p and V at any point on the ion current characteristic in solving for N_p . Practically, however, one must use the ion current at a point in the dumbbell volt-ampere characteristic at which the voltage of the hemisphere can be calculated. Such a voltage is the so-called electron cutoff potential which is defined as the point on the volt-ampere characteristic where the extrapolated positive ion current just begins to deviate from the net current (see Figure 15). At this point, the electron current reaches about one percent of the ion current. From the current equations, this corresponds to a hemisphere potential, V , of approximately ten times the voltage equivalent of temperature, V_0 . Where $V_0 = \frac{kT_e}{e}$. Thus

eV/kT , the remaining variable in (6.2), takes on a value of approximately 10. Fortunately, again, the ion current is not a strong function of voltage so that an error in this approximation is not serious.

In summary, then, the procedure for calculating the positive ion density is quite straight-forward. First, one extrapolates the ion current characteristic with a straight line, locates the point of deviation of the line from the net current curve, and then observes the measured current, i_p cutoff, at this point. Having determined the orientation, velocity, and temperature, calculated the potential, and assumed an ion mass, the positive ion number density is found by solving (6.2).

7.0 CONCLUDING REMARKS

The careful reader will recognize that the equations developed here for the current to a hemispherical collector do not strictly represent the actual characteristics of such a collector in the ionosphere. Simplifying assumptions concerning the initial velocities of the particles, the shape of the sheath, and the presence of electrons in the sheath will each introduce some error into the expression. However, as indicated in the text, these assumptions introduce relatively small perturbations in the current equations and thus will not significantly change the interpretation of ionosphere data as obtained from Dumbbell probe characteristics. Theoretical work toward including these effects in a more exact theory is being pursued.

Several Dumbbell probes have been launched over the past few years^{4,16} and have yielded many ionosphere-electron-temperature and positive-ion-density profiles up to 420 km. More measurements of this nature are planned for the years immediately ahead, and these will be reported in the literature as the data become available.

8.0 ACKNOWLEDGMENTS

The authors would like to express their appreciation to the following people who have contributed time, energy, and thought to make this report possible: Hugo DiGiulio, for programming the current equations and preparing figures; Yui-may Chang and Akira Yokoi, for plotting graphs; Madhoo Kanal, especially, who initiated the study of the moving Dumbbell current equations and is carrying on the study of the general current equations of moving bodies; and Rosann Burke and Jacqueline Delaverdac, for typing the manuscript.

9.0 REFERENCES

1. Hok, G., Spencer, N.W., and Dow, W.G., "Dynamic Probe Measurements in the Ionosphere," J. Geo. Res., 58, No. 2 (1953).
2. Hok, G., Spencer, N.W., Dow, W.G., and Reifman, A., Dynamic Probe Measurements in the Ionosphere, Univ. of Mich. Eng. Res. Inst. Report, Ann Arbor, August, 1951.
3. Reifman, A., and Dow, W.G., "Theory and Application of the Variable Voltage Probe for Exploration of the Ionosphere," Phys. Rev., 75, 1311 A (1949).
4. Boggess, R.L., Brace, L.H., and Spencer, N.W., "Langmuir Probe Measurements in the Ionosphere," J. Geo. Res. 64, 1627 (1959).
5. Carignan, G.R., and Brace, L.H., The Dumbbell Electrostatic Ionosphere Probe: Engineering Aspects, Univ. of Michigan ORA Report No. 03599-6-S, Ann Arbor.
6. Boggess, R.L., Theoretical Considerations in Design of an Ionospheric Probe, Univ. of Mich. Res. Inst. Report FS-2, Ann Arbor, Feb., 1959.
7. Boggess, R.L., Electrostatic Probe Measurements of the Ionosphere, Univ. of Mich. Res. Inst. Report GS-1, Ann Arbor, Nov., 1959.
8. Langmuir, I., and Compton, K.T., "Electrical Discharges in Gases," Rev. Mod. Phy., 3, 191 (1931).
9. Mott-Smith, H.M., and Langmuir, I., "The Theory of Collectors in Gaseous Discharges," Phy. Rev., 28, 727 (1926).
10. Johnson, E.O., and Malter, L., "A Floating Double Probe Method for Measurements in Gas Discharges," Phys. Rev., 80, 58 (1950).
11. Koyiuna, S., and Takayana, K., J. Phys. Soc. Japan, 4, 349 (1949).
12. Brace, L.H., Transistorized Circuits for Use in Space-Research Instrumentation, Univ. of Mich. Res. Inst. Report, Ann Arbor, Oct. 1959.
13. Nicolet, M., "Helium, an Important Constituent in the Lower Exosphere," J. Geo. Res., 66, 2263 (1961).

14. Hanson, W., and Johnson, F.S. "Electron Temperatures in the Ionosphere," Tenth Int. Astrophysical Colloquium, Liege, Belgium, 1961.
15. Chopra, K.P., "Interactions of Rapidly Moving Bodies in Terrestrial Atmosphere," Rev. Mod. Phys., 33, 153 (1961).
16. Spencer, N.W., Brace, L.H., and Carignan, G.R., "Electron Temperature and Thermal Equilibrium in the Ionosphere," J. Geo. Res., in press.
17. Hinteregger, H.E., and Damon, K.R., "Analysis of Photoelectrons from Solar Extreme Ultraviolet," J. Geo. Res. 64, 961 (1959).
18. Johnson, C.Y., Meadows, E.B., and Holms, J.C., "Ion Composition of the Artic Ionosphere," J. Geo. Res., 63, 443 (1958).
19. Taylor, H.A., and Brinton, H.C., "Atomospheric Ion Composition Measured above Wallops Island, Virginia," J. Geo. Res., 66, 2587 (1961).

APPENDIX I

Derivation of the Random Current Density to a Moving
Infinitesimal Area Element

The random current density to an area element is found by integrating the current flux over all allowed velocities.

$$j_x = \frac{Nec}{\pi^{3/2} \lambda_x} \iiint (v_x + \lambda_x) \exp(-v^2) dv_x dv_y dv_z \quad (1)$$

The quantity $(v_x + \lambda_x)$ is the relative velocity between an area element and a particle. The range of allowed velocities is found by the condition that a particle have sufficient normal velocity (v_x) to overtake the moving area and any tangential velocity.

$$0 < v_x + \lambda_x < \infty, \quad -\infty < v_y, v_z < \infty \quad (2)$$

The integration of (1) is based on the following three integrals.

$$\int_{-\infty}^{\infty} dt \exp(-t^2) = \sqrt{\pi} \quad (3)$$

$$\int_{-\lambda_x}^{\infty} v_x dv_x \exp(-v_x^2) = \frac{1}{2} \exp(-\lambda_x^2) \quad (4)$$

$$\lambda_x \int_{-\lambda_x}^{\infty} dv_x \exp(-v_x^2) = \frac{\sqrt{\pi}}{2} \lambda_x (1 + \operatorname{erf} \lambda_x) \quad (5)$$

Thus the random current density to a moving area element is

$$j_x = \frac{Nec}{2\sqrt{\pi}} \left\{ \sqrt{\pi} \lambda_x (1 + \operatorname{erf} \lambda_x) + \exp(-\lambda_x^2) \right\} \quad (6)$$

Note that the current is a function of the velocity component normal to the area element, so that the velocity factor varies with $\lambda \cos \theta$, where θ

is the angle between the velocity vector $\vec{\lambda}$, ($\lambda = \frac{1}{c} \vec{w}$) and the area normal. The current density to an area element having an arbitrary orientation in space but whose normal vector makes an angle θ with respect to $\vec{\lambda}$ is

$$j_{\theta} = \frac{Nec}{2\sqrt{\pi}} \left\{ \sqrt{\pi} \lambda \cos \theta (1 + \operatorname{erf}(\lambda \cos \theta)) + \exp(-\lambda^2 \cos^2 \theta) \right\} \quad (7)$$

APPENDIX II

The Random Ion Current to a Moving Hemisphere

The random ion current to a hemisphere moving with velocity \vec{w} and oriented at an angle θ (Figure 16) is found by integrating the current density to an area element of the hemisphere over its surface.

$$i = \iint a^2 \sin \psi d\psi d\phi j_{\psi} \quad (1)$$

Where $a^2 \sin \psi d\psi d\phi$ is the surface element, and j_{ψ} is the current density given by (7) of Appendix I. To facilitate the integration, the hemisphere is decomposed into two segments.

$$1 \quad 0 < \phi < 2\pi, \quad 0 < \psi < \frac{\pi}{2} - \theta \quad (2)$$

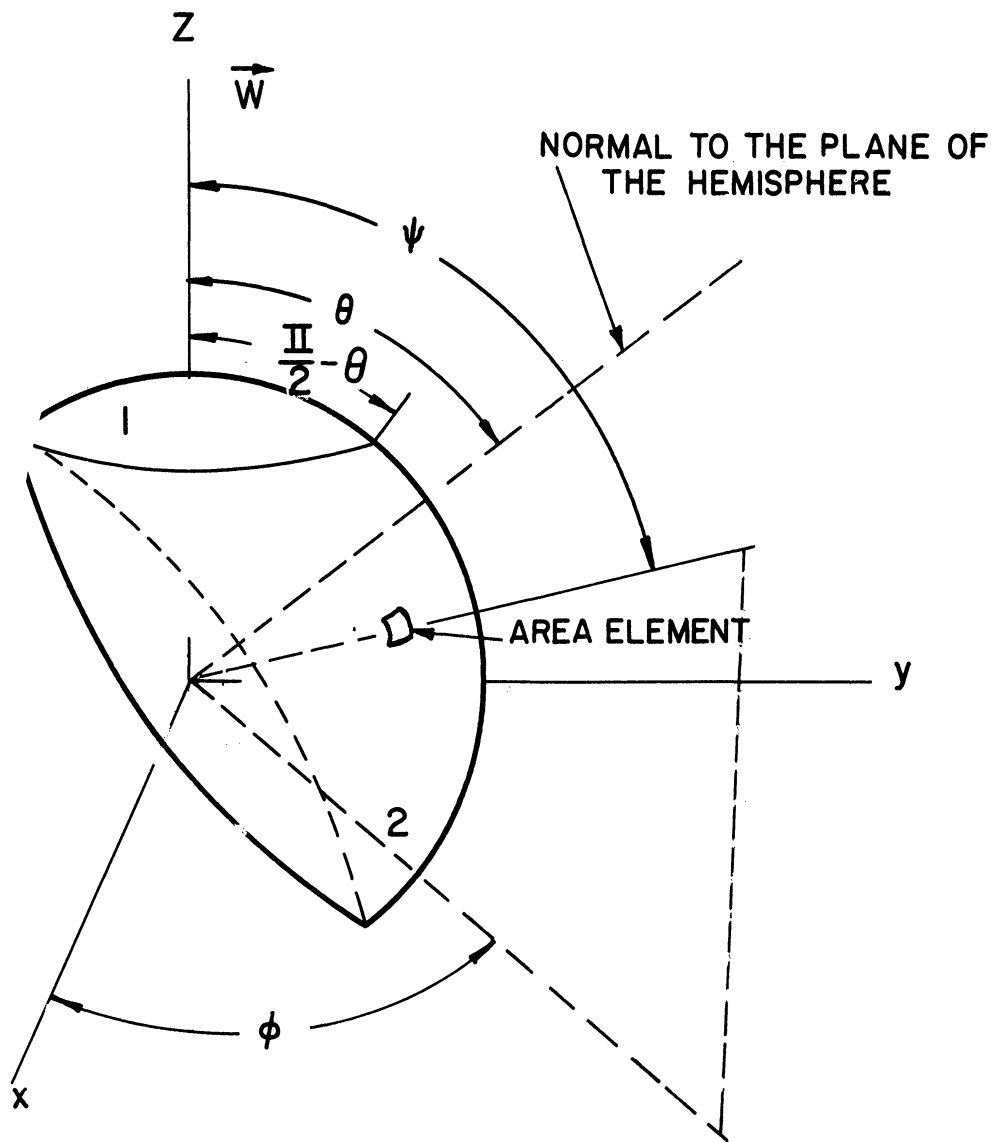
$$2 \quad \phi_0 < \phi < \frac{\pi}{2}, \quad \frac{\pi}{2} - \theta < \psi < \frac{\pi}{2} + \theta \quad (3)$$

ϕ_0 is defined as the value taken by ϕ at the hemisphere edge at a latitude ψ and is given by

$$\phi_0 = -\arcsin(\cot \theta \cot \psi) \quad (4)$$

The current equals the sum of the following two integrals resulting from the two segments

$$i = I_1 + I_2 \quad (5)$$



ψ = LATITUDE ANGLE

ϕ = AZIMUTH ANGLE

Figure 16. Hemisphere orientation.

where

$$I_1 = \int_0^{2\pi} d\phi \int_0^{\frac{\pi-\theta}{2}} a^2 \sin \psi d\psi j_\psi = 2\pi a^2 \int_0^{\frac{\pi-\theta}{2}} d\psi \sin \psi j_\psi \quad (6)$$

and

$$I_2 = 2 \int_{\phi_0}^{\frac{\pi}{2}} d\phi \int_{\frac{\pi-\theta}{2}}^{\frac{\pi+\theta}{2}} a^2 \sin \psi d\psi j_\psi = 2a^2 \int_{\frac{\pi-\theta}{2}}^{\frac{\pi+\theta}{2}} \left[\frac{\pi}{2} + \arcsin(\cot \theta \cot \psi) \right] \sin \psi d\psi j_\psi \quad (7)$$

Let I_{21} and I_{22} represent the terms of (7) without and with the arcsine function, respectively. Consider the integral

$$\begin{aligned} F(x) &= \int_0^x dt j(t) = \frac{Nec}{2\sqrt{\pi}} \int_0^x dt \left\{ \sqrt{\pi} t(1 + \operatorname{erf} t) + \exp(-t^2) \right\} \quad (8) \\ &= \frac{Nec}{2\sqrt{\pi}} \left\{ \sqrt{\pi} \left(\frac{x^2}{2} + \frac{1}{4} \right) \operatorname{erf} x + \frac{x}{2} \exp(-x^2) + \frac{\sqrt{\pi}}{2} x^2 \right\} \end{aligned}$$

With (8) the evaluation of I_1 and I_{21} is carried out with the substitution

$$\begin{aligned} t &= \lambda \cos \psi \\ I_1 + I_{21} &= -\frac{2\pi a^2}{\lambda} \int_{\lambda}^{\lambda \sin \theta} dF(t) - \frac{2\pi a^2}{2\lambda} \int_{\lambda \sin \theta}^{-\lambda \sin \theta} dF(t) \\ &= \frac{2\pi a^2}{\lambda} F(\lambda) - \frac{2\pi a^2}{\lambda} \frac{Nec}{2\sqrt{\pi}} \frac{\sqrt{\pi}}{2} \lambda^2 \sin^2 \theta \quad (9) \end{aligned}$$

With the same substitution I_{22} is represented by

$$I_{22} = -\frac{2a^2}{\lambda} \frac{Nec}{2\sqrt{\pi}} \int_{\lambda \sin \theta}^{-\lambda \sin \theta} dt \arcsin \left(\frac{t \cot \theta}{\sqrt{\lambda^2 - t^2}} \right) \left\{ \sqrt{\pi} t(1 + \operatorname{erf} t) + \exp(-t^2) \right\} \quad (10)$$

Over an even interval only the even part of the integrand contributes to (10)

so that it simplifies to

$$I_{22} = -\frac{2a^2}{\lambda} \frac{Nec}{2\sqrt{\pi}} \int_{\lambda \sin \theta}^{-\lambda \sin \theta} dt \sqrt{\pi} t \arcsin \left(\frac{t \cot \theta}{\sqrt{\lambda^2 - t^2}} \right) \quad (11)$$

Transform I_{22} back to the variables ψ and λ and integrate by parts

$$\begin{aligned} I_{22} &= \frac{Nec}{2\sqrt{\pi}} 2a^2 \sqrt{\pi} \int_{\frac{\pi-\theta}{2}}^{\frac{\pi+\theta}{2}} d\psi \sin \psi \lambda \cos \psi \arcsin(\cot \theta \cot \psi) \\ &= \frac{Nec}{2\sqrt{\pi}} 2a^2 \lambda \sqrt{\pi} \left[-\frac{\pi}{2} \cos^2 \theta + \frac{\cot \theta}{2} \int_{\frac{\pi-\theta}{2}}^{\frac{\pi+\theta}{2}} \frac{d\psi}{\sqrt{1 - \cot^2 \theta \cot^2 \psi}} \right] \quad (12) \end{aligned}$$

In the remaining integral make the substitution $x = \frac{\cos\psi}{\sin\theta}$

$$\frac{\cot\theta}{2} \int_{\frac{\pi}{2}-\theta}^{\frac{\pi}{2}+\theta} \frac{d\psi}{\sqrt{1 - \cot^2\theta \cot^2\psi}} = \frac{\cos\theta}{2} \int_{-1}^1 \frac{dx}{\sqrt{1 - x^2}} = \frac{\pi}{2} \cos\theta \quad (13)$$

The ion current is found by adding together (9) and (12) and simplifying with (8) and (13),

$$i = \frac{Nec}{2\sqrt{\pi}} 2\pi a^2 \left[\frac{\sqrt{\pi}}{2} \left(\lambda + \frac{1}{2\lambda} \right) \operatorname{erf} \lambda + \frac{1}{2} \exp(-\lambda^2) + \frac{\sqrt{\pi}}{2} \lambda \cos\theta \right] \quad (14)$$

It is seen that the current is equal to the random ion current to a stationary hemisphere multiplied by the velocity factor

$$\Lambda(\lambda, \theta) \equiv \frac{\sqrt{\pi}}{2} \left(\lambda + \frac{1}{2\lambda} \right) \operatorname{erf} \lambda + \frac{1}{2} \exp(-\lambda^2) + \frac{\sqrt{\pi}}{2} \lambda \cos\theta \quad (15)$$

In the limit of zero velocity, the factor Λ reduces to unity. The asymptotic form of Λ for large velocity is

$$\Lambda(\lambda, \theta) \underset{\lambda \rightarrow \infty}{\sim} \sqrt{\pi} \left(\frac{1 + \cos\theta}{2} \right) \lambda \quad (16)$$

so that in this limit the current reduces to the product of charge density N_e , probe velocity w , and projected area of the hemisphere in the direction of motion $a^2(1+\cos\theta)/2$.

APPENDIX III

Electron Current to a Hemisphere

The electron current is found from the same integral which defines the positive ion current, (1) of Appendix I, except that λ is essentially zero and the range of allowed velocities is different. Since electrons are retarded (assuming a negative hemisphere), they will reach the probe surface only when their energy exceeds the repulsive energy. Thus energy and momentum

considerations determine the velocity limits⁷

$$\sqrt{\frac{eV}{kT}} < v_x < \infty, \quad 0 < v_y^2 + v_z^2 < \frac{v_x^2 + \frac{eV}{kT}}{\frac{a^2}{r^2} - 1} \quad (1)$$

Integration over these limits gives the electron current density

$$j_e = \frac{Nec}{2\sqrt{\pi}} \frac{r^2}{a^2} \exp\left(-\frac{eV}{kT}\right) \quad (2)$$

The electron current is obtained by multiplying the current density by the sheath area $2\pi a^2$

$$i_e = \frac{N_e e c_e}{2\sqrt{\pi}} 2\pi r^2 \exp\left(-\frac{eV}{kT_e}\right) \quad (3)$$

This current has the simple interpretation of being the random current at the probe surface

$$i_e = \frac{N_r e c}{2\sqrt{\pi}} 2\pi r^2 \quad (4)$$

where N_r is the number density of electrons at the probe and is related to the plasma density N by the Maxwell-Boltzmann relation.

$$N_r = N \exp\left(-\frac{eV}{kT}\right) \quad (5)$$

APPENDIX IV

Derivation of the Second Ion Current Equation Through a Solution of Poisson's Equation

Poisson's equation is integrated using a simple relation between current density, charge density, and potential which asserts that ions enter the sheath with zero velocity and that no electrons are present in the sheath. Thus the particle velocity is determined by the accelerating field, and the current density is due only to ion flow.

$$j = \rho \sqrt{\frac{2eV}{m_p}} \quad (1)$$

Inserting (1) into Poisson's equation (2a)

$$\Delta V = \rho/\epsilon_0 \quad (2a)$$

gives the nonlinear partial differential equation (2b),

$$\Delta V = j \frac{1}{\epsilon_0} \sqrt{\frac{m_p}{2e}} V^{-1/2} \cdot \quad (2b)$$

Under equilibrium conditions the current density is divergence-free

$$\frac{1}{r^2} \frac{d}{dr} r^2 j = 0 \quad (3)$$

It is asserted that the form of the solution of (2) is similar to the one-dimensional solution so that

$$j = \frac{4}{9} \epsilon_0 \sqrt{\frac{2e}{m_p}} \frac{V^{3/2}}{r^2 \alpha^2} \quad (4)$$

where α is some function of r which is determined by solving (2). Substitute (4) into (2)

$$\Delta V = \frac{4}{9} \frac{V}{r^2 \alpha^2} \quad (5)$$

Substituting (4) into the divergence condition gives

$$\frac{d}{dr} \frac{V^{3/2}}{\alpha^2} = 0 \quad \text{or} \quad \frac{3dV}{V} = \frac{4d\alpha}{\alpha} \cdot \quad (6)$$

V is eliminated from (5) by substituting α for V according to (6). The result is a differential equation satisfied by α ,

$$3\alpha r^2 \frac{d^2\alpha}{dr^2} + r^2 \left(\frac{d\alpha}{dr}\right)^2 + 6\alpha r \frac{d\alpha}{dr} = 1 \cdot \quad (7)$$

Thus, Poisson's equation has been solved since α can be found in terms of a general radius r from (7). The positive ion current is obtained by multiplying the current density (4) by the hemispherical collector area, $2\pi r^2$ (note that jr^2 is a constant so j is the current density at the probe when r is the fixed probe radius).

$$i_p = \frac{4}{9} \epsilon_0 \sqrt{\frac{2e}{m_p}} 2\pi \frac{V^{3/2}}{\alpha^2} \quad (8)$$

The ion current is transformed to the more familiar form by substituting

$$P = \frac{8\sqrt{\pi}\epsilon_0 kT}{9e^2 N r^2} \quad \text{and} \quad c = (2kT/m)^{1/2} \quad \text{into (8):}$$

$$i_p = \frac{N_p e c_p}{2\sqrt{\pi}} 2\pi r^2 \frac{P}{\alpha^2} \left(\frac{eV}{kT}\right)^{3/2} \quad (9)$$

APPENDIX V

Relation Between Probe Potential and Sheath Radius

Inversion of the relation between probe potential and sheath radius [Eq. (3.17)] results in a power series expressing a^2/r^2 as a function of V . This is carried out by a change of variables in the equation defining α in Appendix IV, Eq. (7). This differential equation may be written in a form in which α depends on a/r rather than a alone.

$$3\alpha\left(\frac{a}{r}\right)^2 \left(\frac{d}{d\frac{a}{r}}\right)^2 \alpha + \frac{a^2}{r^2} \left(\frac{d\alpha}{d\frac{a}{r}}\right)^2 + 6\alpha \frac{a}{r} \frac{d\alpha}{d\frac{a}{r}} = 1 \quad (1)$$

Consider the change of variables,

$$g = \frac{a^2}{r^2}, \quad x = \alpha \frac{a}{r} \quad (2)$$

with g considered a function of x , and $g' = dg/dx$. Transform the differentials of (1) into x and g ,

$$\frac{d\alpha}{d\frac{a}{r}} = \frac{dx}{d\frac{a}{r}} \frac{d\alpha}{dx} = \frac{2}{g'} - \frac{x}{g} \quad (3)$$

$$\left(\frac{d}{d\frac{a}{r}}\right)^2 \alpha = \frac{dx}{d\frac{a}{r}} \frac{d}{dx} \left(\frac{2}{g'} - \frac{x}{g}\right) = \frac{2g^{1/2}}{g'} \left(\frac{xg'}{g^2} - \frac{1}{g} - \frac{2g''}{g'^2}\right) \quad (4)$$

Substitution of (2), (3), and (4) into (1) yields a differential equation satisfied by $g(x)$

$$\frac{x^2}{g} + \frac{2x}{g'} - \frac{12xg''g}{g'^3} + \frac{4g}{g'^2} = 1 \quad (5)$$

or

$$12 x g''g^2 - 2 x gg'^2 - x^2g'^3 - 4g^2g' + gg'^3 = 0 \quad (6)$$

In solving (6) assume the power series form

$$g(x) = A + Bx + Cx^2 + Dx^3 + \dots \quad (7)$$

Set $A = 1$ to satisfy the boundary condition that the sheath shrink to the probe surface when the probe potential becomes zero. It is found that the solution is

$$g(x) = 1 + 2x + \frac{3}{5}x^2 - \frac{17}{300}x^3 + \dots \quad (8)$$

Using the relation between x and the potential,

$$x = \sqrt{\frac{P}{\Lambda}} \left(\frac{eV}{kT} \right)^{3/4} \quad (9)$$

found by equating (14) of II and (9) of IV, it is seen that the sheath size a^2/r^2 is related to the potential V by

$$\frac{a^2}{r^2} = 1 + 2\sqrt{\frac{P}{\Lambda}} \left(\frac{eV}{kT} \right)^{3/4} + \text{higher order terms.} \quad (10)$$

The error introduced by neglecting higher-order terms is considered less than the error introduced by the assumption used in solving Poisson's equation viz., that ions are emitted with zero initial velocity at the sheath edge.

APPENDIX VI

Comment on the Effect of Velocity on the Electron Current

The remarks in section 3.2 are not to be interpreted as a claim that the electron current to a particular area element on a moving body will experience no change as a result of the motion. Indeed, the complicated sheath distortions which may result from the high velocity of the body could cause readily detectable changes in the electron current, particularly at the trailing surfaces; but these would result primarily from changes in the electrostatic forces in the sheath rather than the modification of the electron velocity distribution relative to the collector, the only effect considered in section 3.2.

UNIVERSITY OF MICHIGAN



3 9015 03025 2608